Máster Interuniversitario en Física Nuclear

UNIVERSIDAD DE SEVILLA

PROPAGATION OF ERRORS IN NUCLEAR DATA TO REACTOR PARAMETERS

CIEMAT
Unidad de Innovación Nuclear
División de Fisión Nuclear - Dpto. Energía

Master thesis

Author:
José Llanes Gamonoso

Thesis directors:
Vicente Bécares Palacios, Francisco Álvarez Velarde,
Carlos Guerrero Sánchez

June 2022

*A mi familia y amigos, por su apoyo
incondicional.
A Vicente y Paco, por la oportunidad y la
confianza dada para hacer este trabajo.*

Abstract

The knowledge of reactor parameters such as effective multiplication factor k_{eff}, effective delayed neutron fraction β_{eff} and their uncertainties is important for the study of nuclear reactor dynamics and for nuclear reactor safety analysis. In this work we will do a S/U analysis with the SUMMON code, based on first order perturbation theory, of several simulations performed with Monte Carlo code MCNP for 25 benchmark reactors, mainly from ICSBEP and IRPhE reactor databases. In the case of k_{eff}, it has been found that the uncertainty due to nuclear data is much larger than the statistical uncertainties from the Monte Carlo method. On the other hand, the evaluation of β_{eff} with the conventional method (Bretscher's method) has non negligible statistical uncertainties. A perturbative method will be used (Chiba's method) to improve statistical uncertainties. Three covariance matrices from three different nuclear data libraries will be used for the uncertainty analysis: JEFF-3.3, JENDL-4.0u and ENDF/B-VIII.0.

For the k_{eff}, we have observed a good statistical convergence and a wide range of reaction contributors in the uncertainty due to nuclear data, which is usually larger with JEFF-3.3 library. For β_{eff}, Chiba's method appears as the best method due to the improvement in statistical uncertainty and the removal of false contributors in the uncertainty due to nuclear data, being $\bar{\nu}_d$ the nuclear data with the most important contribution. In general, JENDL-4.0u has been found to be the best library for the uncertainty evaluation for β_{eff}.

Resumen

El conocimiento de los parámetros de los reactores como el factor de multiplicación efectivo k_{eff}, la fracción de neutrones retardados efectiva β_{eff} y sus incertidumbres es importante para el estudio de la dinámica y el análisis de seguridad de los reactores nucleares. En este trabajo haremos un análisis S/U con el código SUMMON, basado en la teoría de perturbación de primer orden, de varias simulaciones realizadas con el código de Monte Carlo MCNP para 25 reactores de referencia, principalmente provenientes de las bases de datos de reactores ICSBEP y IRPhE. En el caso de k_{eff}, se ha encontrado que las incertidumbres debidas a datos nucleares son mucho mayores que las incertidumbres estadísticas del método de Monte Carlo. Por otro lado, el cálculo de β_{eff} con el método convencional (método de Bretscher) tiene unas incertidumbres estadísticas no despreciables. Usaremos un método perturbativo (método de Chiba) para mejorar las incertidumbres estadísticas. Tres matrices de covarianzas de tres librerías de datos nucleares distintas serán usadas para el análisis de la incertidumbre: JEFF-3.3, JENDL-4.0u y ENDF/B-VIII.0.

Para la k_{eff}, hemos observado una buena convergencia estadística y un amplio rango de contribuyentes a la incertidumbre debida a datos nucleares, la cual es normalmente mayor con la librería JEFF-3.3. Para la β_{eff}, el método de Chiba aparece como el mejor método debido a la mejora en la incertidumbre estadística y la eliminación de los falsos contribuyentes a la incertidumbre debida a datos nucleares, siendo $\bar{\nu}_d$ el dato nuclear con la contribución más importante. En general, JENDL-4.0u ha sido encontrada como la mejor librería para la evaluación de las incertidumbres para la β_{eff}.

Contents

1 Introduction and motivation

Nuclear energy is an important source of energy in some of the main developed countries. The first prototypes of nuclear reactors date from the middle of twentieth century (USA). We can find the first commercial reactors in the 1950s and 1960s that we call in our days Generation I. The majority of the reactors operating nowadays are known as Generation II and include a wide range of technologies such as BWR, PWR, CANDU, RBMK, etc. Spain counts currently with seven reactor units in an operational status (Pressure Water Reactor and Boiling Water Reactor) that, according to IAEA [1], generated 55609 GWh (the 21.2% of total production) in 2017. Spain has also three reactor units in a permanent shutdown status.

Nuclear technology is being considered as one of the fundamental tools in the fight against climate change. To consider the impact of nuclear energy in nature properly, we have to take into account the whole nuclear power fuel cycle: uranium mining, uranium conversion and enrichment, fuel fabrication, power generation, used fuel management and waste management. Concerning CO_2 emissions, the estimations is at 5.5 g CO_2 eq./kWh [2], a value comparable with the renewable range. On the other hand, and contrary to popular belief, this kind of energy is not only one of the cleanest but one of the safest together with renewable energy. To check some data about that question, see reference [3].

Now, the future of fission nuclear energy is focused on the development of new nuclear fuel cycles and advanced systems with more efficiency in fuel utilization, that can reduce the levels of radioactive waste produced to be confined in geological repositories, and with even better safety standards and reduced proliferation risks. One of these systems is the Accelerator Driven sub-critical System (ADS) for nuclear waste transmutation, which is based on a sub-critical reactor with a spallation neutron source provided by a high power-accelerator. Other ones are Generation IV reactors, which include several technologies like very-high-temperature reactor (VHTR), molten salt reactor (MSR), lead-cooled fast reactor (LFR), supercritical-water-cooled reactor (SCWR), sodium-cooled fast reactor (SFR) and gas-cooled fast reactor (GFR). The last two could allow the reuse of the spent nuclear fuel by its reprocessing. Another new concept is the Small Modular Reactor (SMR) that is based in the technologies previously mentioned. It is characterized by reactors under 300 MW of electric power and the possibility to transport and install them in different locations. They are expected to let access to nuclear energy to countries and regions that cannot count currently with this technology. As mentioned before, these new systems are under development. In this stage, it is very important to perform computer simulations (for example, with Monte Carlo codes) to obtain information about the behaviour and dynamics of these new designs.

To characterize this behaviour, we are interested in the evaluation of the major reactor parameters and its errors due to nuclear data, which is the main theme of this thesis. These parameters are mainly three: the multiplication factor k is the ratio between the number of neutrons produced in fission and the number of neutrons lost; the delayed neutron fraction β is the fraction of neutrons produced and emitted in the decay of the fission fragments; and the mean generation time Λ is the mean time between the birth of a neutron and the absorption-inducing fission.

In order to obtain a reliable evaluation of these key parameters, it is very important to do efforts in the improvement and development of libraries of evaluated nuclear data, new models and simulation tools.

With respect to the propagation of uncertainties, it is necessary to have into account the different sources of errors that we can find in the calculations. In our case, we have two different sources: statistical errors, when Monte Carlo codes are used for our simulations, and errors due to propagation of uncertainties in the nuclear data. In principle, we can reduce statistical errors in our simulation error by increasing the simulation time (depending on the simulated system and/or the computation capabilities we have, this is more or less difficult). Hence, the main source of errors are usually the nuclear data uncertainties. In spite of the importance of these errors in reactor physics simulations, significant gaps between the current uncertainties and the target accuracies (maximum acceptable uncertainties due to nuclear data for a certain parameter as agreed by the industry, regulation and research communities) are found [4]. European research projects like CHANDA [5] and SANDA [6] aimed to prepare methodologies, facilities, detector, interpretation and tools to face the challenges in the field of nuclear data for nuclear applications. This work is included in task 4.4 of SANDA project [7]. To know more about perspectives and needs about nuclear data applications, see reference [8]. To do the uncertainty propagation due to nuclear data, we work with reliable and flexible calculation codes, in our case, we will use the SUMMON code developed at Ciemat [9].

In chapter two of this work, we will introduce the theoretical basis where we will explain the concept of cross section, taking some time in the particular interesting case of fission (an important input parameter for the reactor response); what is an evaluated nuclear data library, how it is organized and several examples. We will follow with the explanation of what a nuclear reactor is and basic definitions in reactor physics, which will be fundamental for introducing the major reactor parameters along with a brief example of reactor dynamics that will show us the main role of these parameters. In chapter three, we will discuss the concepts of sensitivity and uncertainty analysis, the theory we used for the propagation of errors (first order perturbation theory and the Sandwich Rule), introducing here relevant definitions like sensitivity coefficient and covariance matrix, and how we can calculate the major parameters and sensitivity profiles needed to propagate the errors due to nuclear data using MCNP code outputs and the SUMMON code. Next, we will talk about integral experiments and reactor databases, where we can find the information of the benchmark experiments used in this work.

In chapter four, we will do a brief introduction of the different experiments simulated in the thesis and we will explain the general proceeding followed since the input of the MCNP code until the final uncertainty results. In chapter five, we will present our results and the different analysis we performed on then and, in chapter six, we will extract our final conclusions based on all the previous information and results.

2 Theoretical basis

In this chapter we will introduce basic concepts about nuclear data and their libraries, neutron physics theory and the main reactor parameters that characterize the operation of a nuclear reactor.

2.1 Nuclear data libraries (ENDF, JEFF, JENDL). ENDF format: MF and MT numbers.

In this section, we will focus on the relevant nuclear data in a nuclear reactor context, as well as nuclear data libraries which store these data with their uncertainties, that allow us to perform our nuclear reactor simulations and the propagation of uncertainties.

2.1.1 Cross-sections

Suppose we have an experiment where there are a set of nuclei, named targets, and an incident beam of particles (in this work, we are interested in neutrons). We can write the number of collisions per second like

$$\text{Collisions per second} = \sigma I N V, \tag{2.1.1}$$

where I is the intensity of the beam, N the density of target nuclei and V the volume of the target. The proportionality constant σ is denoted as cross-section and it has units of area. The value of the cross section depends on the nature of the target, (i.e. the isotopes) and the type (i.e. neutrons, protons...) and energy of the incident particles. It is usual to find in reactor equations the product $N\sigma = \Sigma$, which is called macroscopic cross-section. If we consider σ has units of cm^2, then the units of Σ will be cm^{-1}.

Induced Nuclear Fission

Heavy nuclei can suffer spontaneous fission but, in the context of nuclear technology, we are interested in induced fission by neutrons, which is the process that takes place in nuclear reactors. The fission occurs when the nuclei deforms and splits in two nuclei fragments plus neutrons and gammas. The energy necessary to deform the nucleus is called E_{crit}. When a neutron is absorbed by a nucleus, the resulting nucleus has an energy equal to the binding energy of the last neutron, we denoted by B, plus the kinetic energy of the nucleus.

When $E_{crit} > B$, then we need a neutron whose kinetic energy is above the threshold $E_{crit} - B$ to induce nuclear fission, this type of nuclei is called fissionable (for example, ^{238}U). When $E_{crit} < B$, all neutrons can induce nuclear fission and that kind of nucleus are called fissile (for example, ^{235}U).
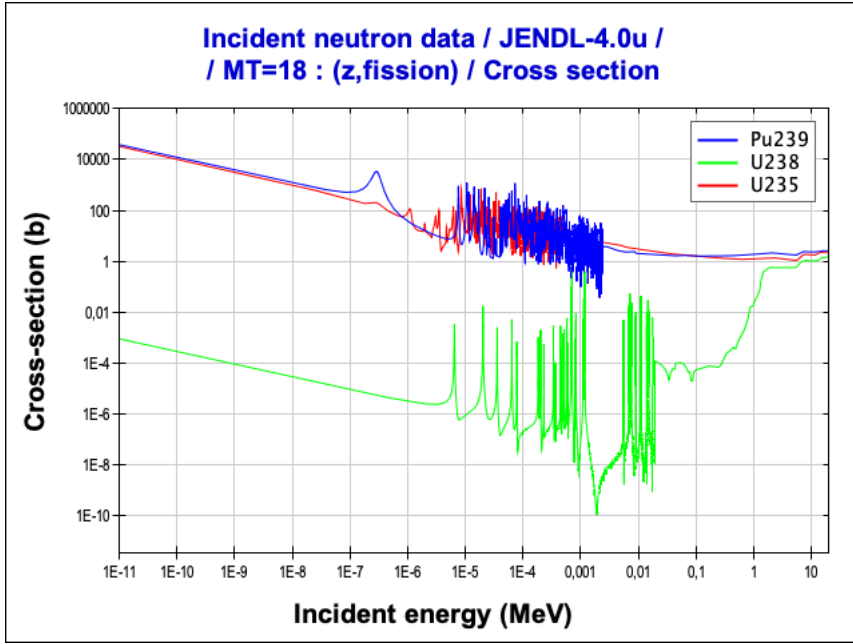
Figure 2.1.1: ^{235}U, ^{239}Pu and ^{238}U cross-sections obtained with [10].

For this reason, we have a non-zero fission cross section for fissile nuclei at low energies, like we can see in figure 2.1.1. In this case, at low energies, the cross-sections follow approximately a $1/v$ dependence, then they suffer some resonances and at high energies is rolling and smooth. It is important here to highlight the fact that the fissile cross section is very large at low energies. By contrast, in fissionable but non-fissile nuclei (figure 2.1.1) cross-sections tend to zero at low energies. In nuclear reactors, the fuel contains fissile and fissionable nuclei.

The induced fission process produces several reaction products. There are a number (usually two) of fission fragments (asymmetrical for low incident neutrons energies and more symmetrical for high incident neutron energies). They are also produced neutrons and gamma rays, that we separate between prompt, emitted at the instant of fission itself, and delayed, emitted at later times by the decay of fission fragments.

In our context, the most interesting fission product is the neutron because is the particle that sustain the chain reaction. The chain reaction is the process in which neutrons produced in one fission induce new fission in other fissile or fissionable nuclei. More than 99% of the neutrons are emitted at the moment of the fission (prompt neutrons) and less than 1% are emitted by nucleus produced on the β-decay of certain fission fragments (delayed neutrons). These fission fragments are called delayed-neutron precursors. The delayed neutron can be arranged into several groups (six groups in ENDF/B and eight in JEFF, nuclear data libraries), each emitted with an average characteristic half-live of the precursor. In spite of representing a tiny percentage in the amount of neutrons, we will see that delayed neutrons are very important in the reactor behaviour and let us control it.

Taking into account both prompt and delayed neutrons, we can denote the average number of neutrons produced in fission by ν. To calculate the neutrons emitted in fission per neutron absorbed, we use the following equation

$$\eta = \nu \frac{\sigma_f}{\sigma_a} = \nu \frac{\sigma_f}{\sigma_\gamma + \sigma_f} \tag{2.1.2}$$

where σ_f, σ_a and σ_γ are respectively the fission, absorption and radiative capture cross-sections. There are more reactions that compete against fission but, for simplicity, we only take into account radiative capture.

2.1.2 Evaluated nuclear data and the ENDF format

Nuclear data (such as cross sections) are essential for any application that requires particle transport calculations and interaction through materials. Nuclear data evaluation is the process in which existing experimental data are combined with results of nuclear models to produce standardized, quality controlled and validated nuclear data libraries that can be used by nuclear calculation codes. Some recent evaluations also include information about the uncertainty in the nuclear data and the correlations between energy ranges and/or different reaction cross sections.

Let us see some examples of nuclear data libraries. The ENDF/B library is maintained by the National Nuclear Data Center (NNDC), which was the first in introducing the ENDF format that is usually used by nuclear data libraries. The JEFF is a merger of JEF (Joint European File) and EFF (European Fusion File). It is maintained by the NEA Data Bank of the Organization for Economic Cooperation and Development (OECD). The JENDL (Japanese Evaluated Nuclear Data Library) is maintained by the Japanese Nuclear Data Committee (JNDC) and the Nuclear Data Center at the Japan Atomic Energy Research Institute (JAERI). Both libraries use the ENDF format.

The ENDF (Evaluated Nuclear Data File) is a computer format [11] to organise nuclear data developed by the US Cross Section Evaluation Working Group (CSEWG), published through the National Nuclear Data Center (NNDC) at the Brookhaven National Laboratory. These files contain, among others, nuclear reactor cross-sections, energy and angle distributions in a determined nuclear reaction, the decay mode and spectra from the decay of radioactive nuclei and the errors in these parameters.

In the ENDF format, nuclear data are identified by a set of numbers:

- MAT number defines the isotope (or isomer).

- MF number defines the type of data.

    - **MF=1** descriptive and miscellaneous data
    - **MF=2** resonance data
    - **MF=3** reaction cross section vs energy
    - **MF=4** angular distributions
    - **MF=5** energy distributions
    - **MF=6** energy-angle distributions
    - **MF=7** thermal scattering data
    - **MF=8** radioactivity data

- **MF=9-10** nuclide productiond data
  - **MF=12-15** photon production data
  - **MF=30-36** covariance data

- MT numbers define the cross sections. For example: MT=1 total, MT=2 elastic scattering, MT=4 inelastic scattering, MT=18 fission, MT=102 capture.

In order to have files with a proper size, the data in the libraries are saved in such a way that can be reconstructed into pointwise or multigroup data with tools as NJOY (nuclear data processing code developed at Los Alamos National Laboratory) [11].

2.2 Nuclear reactors and their major parameters: k, β, Λ.

In this section, we deal with the main reactor parameters that characterize the operation of a nuclear reactor. Before that, we will see some previous concepts which will let us understand how a nuclear reactor works.

2.2.1 Previous definitions

Here we are going to introduce the components of a nuclear reactor and provide a classification according to the neutron spectrum.

Components of a Nuclear reactor

A nuclear reactor is a device that is designed to maintain a fission chain reaction in a controlled manner. Now, we are going to introduce the main components of a nuclear reactor: fuel, moderator and coolant. These elements made up the reactor core, usually located in the reactor center. In the core is where the fission energy production in chain reactions is produced.

Fuel contains fissile and fissionable nuclei. To make a reactor critical (see section 2.2.2), it is necessary a certain concentration of fissile material, but the only fissile isotope present in nature is ^{235}U, which represents only a very small fraction of natural uranium (0.72%, the remaining being non-fissile ^{238}U) . Although some types of reactors can achieve criticality with natural uranium (see below), uranium fuel is usually enriched in ^{235}U. Alternatively, the fissile content of the fuel can be increased through conversion of fertile material. Fertile materials are nuclei that are not fissile, but which can produce fissile isotopes from fertile ones through neutron capture (^{239}Pu from ^{238}U or ^{233}U from ^{232}Th, see next section).

The moderator is a material situated in the core whose main purpose is to slow down fission neutron into thermal neutrons. The interest in reducing the neutron energy is that fission cross sections are much larger at thermal energies (see figure 2.1.1). This is mainly achieved through elastic scattering with the moderator material. Energy transfer between neutrons and the nuclei are more efficient for low mass nuclei, therefore light nuclei are the most efficient moderator. Hence, the most commonly used material is hydrogen, in form of light water (H_2O). However, it has the disadvantage of the relatively high capture cross section of hydrogen, which requires the use of enriched fuel. For this reason, other moderators

are also used. Deuterium, in the form of heavy water (D_2O) has the advantage of the small capture cross section of deuterium, which allows fuelling a reactor with natural uranium. On the other hand, it is more expensive than light water, more collisions are necessary to slow down neutrons (resulting in bigger reactors) and tritium is produced, which is radioactive and difficult to manage. Graphite (C), for its part, is cheap and abundant, has a high density and a small capture cross section (also allowing using natural uranium as fuel). On the other hand, its relative high mass (A = 12) requires adding more amount of moderator, resulting again in bigger reactors. Finally, beryllium is also used in some research reactors, in metallic form or as BeO, but it is expensive and toxic.

Not all reactors feature a moderator. Reactors with a moderator have a thermal neutron spectrum and hence are referred as thermal reactors. Reactors lacking a moderator have a fast neutron spectrum and hence are referred as fast reactors.

The coolant is used to remove fission heat from the reactor. According to the combination of moderator and coolant, several reactor families can be defined. Light Water Reactors (LWRs), moderated and cooled by light water, are the most common type of reactor in operation. They can be classified in turn in Pressurized Water Reactors (PWRs) and Boiling Water Reactors (BWRs), depending on whether water is allowed to boil within the reactor or not. Heavy Water Reactors, moderated by heavy water and usually also cooled by it; the most common design being the CANDU of Canadian origin. Graphite moderated reactors are usually cooled by gas, like in the British Magnox and AGR, the French UNGG, and some advanced concepts such as the HTR (High Temperature Reactor) and PBMR (Pebble Bed Modular Reactor) designs, but also by water in some designs like the Soviet RBMK.

Fast reactors cannot use light materials as coolant and hence fast reactors are cooled by liquid metals (Liquid Metal Fast Reactors, LMFRs), most commonly Na (Sodium Fast Reactors, SFR), or Pb/Pb – Bi (Lead Fast Reactors, LFR), or gas (because of its low density, it does not have a relevant moderating effect (Gas Fast Reactors, GFRs). These coolants make fast reactors more complex than thermal reactors, and furthermore they need higher-enriched fuel to reach the critical state. Nevertheless, they are of interest because they offer advantages for breeding and nuclear waste transmutation (see next section). Finally, Molten Salt Reactors (MSRs) are cooled by molten salts. In this type of reactors, the fuel is usually dissolved within the molten salt coolant. These reactors may be thermal (usually moderated with graphite) or fast. Apart from these, other components of nuclear reactors include:

- The reflector is a layer of material that surrounds the core. It is used to reduce neutron leakage; when a neutron reach the reflector, it suffers scattering interactions so that it may return to the core. Hence, the reflector helps us to reduce the amount of fuel required to make a reactor critical.

- The control rods are an adjustable element that we can control in order to modify the k parameter of the reactor (we will see the k in 2.2.2). They usually are composed of a neutron-absorbing material (boron in form of B_4C or AgInCd). Hence, the insertion of the control rods reduces the neutron population and the withdrawal decreases it.

Burner and breeder reactors

As stated above, the only fissile isotope present in nature in non-trace quantities is ^{235}U, which constitutes only 0.72% of the uranium resources. However, the excess neutrons from nuclear fission can be captured in the so called fertile materials to produce new fissile materials (^{239}Pu from ^{238}U or ^{233}U from ^{232}Th). Thus, the conversion factor C is defined as the average number of fissile nuclei that are produced through neutron capture in fertile materials per fissile nuclei consumed. According the value of the conversion factor, reactors can be classified into burner reactors (C<1) and breeder reactors (C>1).

The vast majority of commercial reactors used for energy production are burner reactors. Breeder reactors are usually fast reactors (Fast Breeder Reactors, FBRs), since the absence of a moderator reduces the captures in the core and hence leaves a larger number of neutrons available for captures in fertile materials. With breeder reactors, the humankind would be able to produce electricity with nuclear energy for thousands of years.

It must be stressed, however, that not all fast reactors are breeders, and neither all breeder reactors are fast reactors. In particular, fast spectrum burner reactors are the preferred option for nuclear waste transmutation [1], taking advantage of the fact that the fission/capture ratio is higher with a fast spectrum than with a thermal one, and hence the actinides present in the fuel "burn" (fission) faster. On the other hand, it is possible to design thermal breeders, in particular operating in the thorium cycle (e.g. the LWBR [13]).

Breeding may be homogeneous or heterogeneous. In the first case, fissile and fertile materials are intermixed in the fuel and breeding occurs in the fuel itself. In the second case, breeding occurs in a layer surrounding the core called breeding blanket. Since the materials in the blanket may also undergo fissions, the blanket also needs a coolant. When the desired level of fissile isotopes is achieved, the fuel and/or blanket material are withdrawn from the reactor and a chemical extraction is performed to separate the bred fissile nuclei and new fuel is manufactured from it in a process that is called fuel reprocessing.

Neutron transport

The fundamental problem in the design of a nuclear reactor is to know how the neutron flux is distributed within the reactors and how does it evolves with time. To find an answer to this problem, we can solve the continuity equation using the diffusion theory. Let's start by writing the Fick's law

$$\mathbf{J} = -D\nabla\phi, \tag{2.2.1}$$

where D is called the difussion coefficient and has units of cm, ϕ is the neutron flux and $\mathbf{J}$ is the neutron current density (both with units of $\mathrm{cm}^{-2}\mathrm{s}^{-1}$). The physical meaning of this equation is that there is a net flow of neutrons from the higher neutron density region to the lower density region.

---

[1]The aim of transmutation is reducing the long term radiotoxicity of high level nuclear waste (HLW), consisting essentially of spent nuclear fuel, through the fission of the Pu, Am and other actinides into much shorter lived fission products. This can be achieved with critical reactors, accelerator-driven subcritical systems (ADS) or (less commonly) fusion-driven systems (FDS) [12].

Now, consider an arbitrary volume V within a medium containing neutrons. If there is a net flow of neutrons through the volume, there will be a change in the number of neutrons in V. To take into account this fact, we use the equation of continuity

$$\frac{\partial N}{\partial t} = s - v\Sigma_a N - \nabla \cdot \mathbf{J}, \qquad (2.2.2)$$

where N is the neutron density (number of neutrons in V volume) and v the neutron velocity. Using the relation between neutron density and flux $N = \phi/v$, we can rewrite in terms of the neutron flux

$$\frac{\partial(\phi/v)}{\partial t} = s - \Sigma_a\phi - \nabla \cdot \mathbf{J}, \qquad (2.2.3)$$

where the left hand side is the change in time of the neutron density, s is the source term of neutrons, the second term in the right hand side is the density of neutrons lose in absorption and the third term is the leakage rate, being $\mathbf{J}$ the neutron current density vector. Substituting (2.2.1) into (2.2.3), we obtain the difussion equation for neutrons

$$D\nabla^2\phi - \Sigma_a\phi + s = \frac{\partial(\phi/v)}{\partial t}. \qquad (2.2.4)$$

We can divide this equation by D and obtain

$$\nabla^2\phi - \frac{1}{L^2}\phi + \frac{s}{D} = \frac{1}{D}\frac{\partial(\phi/v)}{\partial t}, \qquad (2.2.5)$$

where the parameter L^2 is defined as

$$L^2 = \frac{D}{\Sigma_a}, \qquad (2.2.6)$$

and it has units of cm^2 and is called the difussion area (and L the difussion length).

The Group-Diffusion Method

Neutrons in reactors are emitted in fission with a continuous energy spectrum and it broadens due to the interaction with the moderator materials. The problem is that many of the reaction parameters we have to take into account are energy-dependent. To analyze the slowing down and diffusion of neutrons in a reactor, we can use the group-diffusion method.

This method consist in dividing the neutron population into N groups with N energy intervals, where their diffusion coefficients and absorption and scattering cross-sections are averaged in the corresponding energy range (by convention, the most energetic group is denoted by $g = 1$ and the least by $g = N$). The flux in one group is defined as

$$\phi_g = \int_g \phi(E)dE. \qquad (2.2.7)$$

We can lose neutrons in one group by absorption or by slow down in elastic scattering. For the absorption, we define the macroscopic group absorption cross section as

$$\Sigma_{ag} = \frac{1}{\phi_g} \int_g \Sigma_a(E)\phi(E)dE. \tag{2.2.8}$$

With respect to the transfer of neutrons into a less energetic group, we define $\Sigma_{h \to g}$, called the macroscopic group transfer cross-section. We can earn neutrons in our group by transfer too, so similarly we define $\Sigma_{g \to h}$. The derivation of the transfer cross-sections are complicated and are not showed in this work.

2.2.2 Multiplication factor: k

Energy in nuclear reactor is produced by way of a fission chain reaction. The chain reaction can be characterized by the multiplication factor k. In the following point, we are going to introduce our first reactor parameter.

One-group reactor equation

Consider a fast reactor with an homogeneous mixture of fuel and coolant. We assume that the reactor is homogeneous. We consider only one group of neutrons, so the diffusion equation for the reactor will be

$$D\nabla^2\phi - \Sigma_a\phi + s = \frac{1}{v}\frac{\partial\phi}{\partial t}. \tag{2.2.9}$$

In the case of a multiplicative system, neutrons are produced in fission reactions and we can write the neutron source as

$$s = \nu\Sigma_f\phi, \tag{2.2.10}$$

where Σ_f is the macroscopic fission cross section and ν the number of neutrons produced in one fission. In order for such a system to stay stable in time, i.e. $\frac{\partial\phi}{\partial t} = 0$, we need that

$$D\nabla^2\phi - \Sigma_a\phi + \nu\Sigma_f\phi = 0. \tag{2.2.11}$$

that is, the numbers of neutrons produced in fission ($\nu\Sigma_f\phi$) should be equal to the number of neutrons lost either by escape ($D\nabla^2\phi$) or capture ($\Sigma_a\phi$). It is customary to define the criticality constant as

$$k = \frac{\nu\Sigma_f\phi}{-D\nabla^2\phi + \Sigma_a\phi}, \tag{2.2.12}$$

i.e. the ratio between the number of neutrons produced in fission (prompt and delayed) and the number of neutrons lost by capture or escape. Alternatively, it can be understood as the ratio between fission neutrons in one generation and the preceding one

$$k = \frac{\text{number of fissions in one generation}}{\text{number of fissions in preceding generation}}. \tag{2.2.13}$$

We can consider an infinite reactor (no neutron losses) and evaluate its k parameter. Using the k definition (2.2.12) and neglecting the leakage term, we obtain the following equation

$$k_\infty = \frac{\nu \Sigma_f \phi}{\Sigma_a \phi} = \frac{\nu \Sigma_f}{\Sigma_a} \qquad (2.2.14)$$

We can observe that the parameter k_∞ only depends on the materials properties. Therefore, we can use this value in a bare reactor made with the same materials.

Defining B^2 (the geometric buckling) as

$$B^2 = \frac{1}{D}\left(\frac{1}{k}\Sigma_f - \Sigma_a \right), \qquad (2.2.15)$$

we can write equation (2.2.11) as

$$\nabla^2 \phi = -B^2 \phi \qquad (2.2.16)$$

We can obtain a relation between k and k_∞. Dividing (2.2.12) by Σ_a, taking into account the definition of k_∞ (2.2.14) and using equation (2.2.16) follows

$$k = \frac{k_\infty}{1 + L^2 B^2} \qquad (2.2.17)$$

It is worthwhile to remark, as we can observe, that k is independent of the neutron flux, that is, a reactor can be critical at any power level.

When we want to increase the power of the reactor, we have to operate the device (for example with control rods) so that we increase the number of fission in consecutive generations until the reactor reach the desired power. This way of operation in named supercritical $k > 1$. To keep this level of power, we operate the reactor in order to get $k = 1$ (the number of fission in consecutive generations remains the same) and when we reach this value we said that the reactor is critical. To reduce the power or shut down the reactor we are interested in $k < 1$ and we say that the reactor is subcritical, i.e. the number of fissions decrease between generations.

2.2.3 Mean generation time and fraction of delayed neutrons: Λ and β

To introduce this two parameters, we are going to consider the following problem based on a reactor with delayed neutrons. Suppose an infinite homogeneous reactor with six groups of delayed neutrons and that all processes are occurring at one neutron energy (one-group calculation). The diffusion equation is

$$\frac{\partial N}{\partial t} = Dv\nabla^2 N - \Sigma_a vN + s. \qquad (2.2.18)$$

Let us define β as the fraction of the fission neutrons are delayed (it depends on the fuel). Using (2.2.14), it follows that $s(\text{prompt neutrons}) = (1 - \beta)k_\infty \Sigma_a vN$ and $s(\text{delayed neutrons}) = \lambda_i C_i$, where C_i is the precursor concentration in atoms/cm^3 and λ_i is the decay constant of one precursors group. Substituting this expressions into (2.2.19)

$$\frac{\partial N}{\partial t} = Dv\nabla^2 N - \Sigma_a vN + (1 - \beta)k_\infty \Sigma_a vN + \sum_{i=1}^{6} \lambda_i C_i + s_0, \qquad (2.2.19)$$

where s_0 are the neutrons not produced in fission. Let us consider that each delayed neutron appears after the decay of one precursor, the production rate of precursors can be written as $\beta k_\infty \Sigma_a v N$. The set of equations that rules the precursor population is ($i = 1, ..., 6$)

$$\frac{dC_i}{dt} = \beta_i k_\infty \Sigma_a v N - \lambda_i C_i. \qquad (2.2.20)$$

We are interested in solving the problem formed by (2.2.19) and (2.2.20). We assume the solutions of N and C_i are separable solutions in space and time (valid only if the reactor is near the critical state and there are no localized perturbations, see reference [14])

$$N(\mathbf{r}, t) = f(\mathbf{r})n(t), \quad C_i(\mathbf{r}, t) = g_i(\mathbf{r})c_i(t). \qquad (2.2.21)$$

Substituting (2.2.21) into (2.2.19) and (2.2.20), it follows

$$\frac{dc_i}{dt} = \beta_i k_\infty \Sigma_a v \frac{f(\mathbf{r})}{g_i(\mathbf{r})} n(t) - \lambda_i c_i(t), \qquad (2.2.22)$$

$$\frac{dn}{dt} = D v \frac{\nabla^2 f}{f} n(t) - \Sigma_a v n(t) + (1 - \beta) k_\infty \Sigma_a v n(t) +$$
$$+ \Sigma_i \lambda_i \frac{g_i(\mathbf{r})}{f(\mathbf{r})} c_i(t) + \frac{s_0}{f}. \qquad (2.2.23)$$

With the hypothesis we made, this last two equations have to be independent of position. For that reason, we assume $f/g_i = 1$ and $s_0/f = q(t)$. Using (2.2.16), we obtain $\nabla^2 f/f = -B^2$, which is a constant.

Let us define the absorption lifetime as

$$\Lambda_\infty = \frac{1}{v\Sigma_a}, \qquad (2.2.24)$$

the mean time a neutron travels before being absorbed. With this definition, we can introduce the neutron lifetime

$$\Lambda_0 = \frac{\Lambda_\infty}{1 + L^2 B^2}. \qquad (2.2.25)$$

the mean time a neutron travels before leakage or being absorbed. We define the mean generation time as

$$\Lambda = \frac{1}{\nu v \Sigma_f} = \frac{1/v}{k_\infty \Sigma_a} = \frac{\Lambda_\infty}{(1 + L^2 B^2)k} = \frac{\Lambda_0}{k}, \qquad (2.2.26)$$

which is understood as the mean time between the birth of a neutron and the absorption-inducing fission. When $k \approx 1$ and there are not delayed neutrons, $\Lambda \approx \Lambda_0^p$, where Λ_0^p is the prompt neutron lifetime, which is defined as the average time between the emission of the prompt neutron and their absorption. The most part of the life of a prompt neutron is like a thermal neutron because to slow down to thermal energies require much less time. Therefore, in an infinite reactor we can write $\Lambda_0^p \approx \Lambda_\infty^t$ where Λ_∞^t is the mean difussion time, the average lifetime of a thermal neutron in an infinite system.

With the mean generation time definition, defining the reactivity[2] as

$$\rho = \frac{k-1}{k},$$ (2.2.27)

and using the diffusion area definition and the equation (2.2.17), we can rewrite our differential equation system as

$$\frac{dn}{dt} = \frac{\rho - \beta}{\Lambda} n + \Sigma_i \lambda_i c_i + q,$$ (2.2.28)

$$\frac{dc_i}{dt} = \frac{\beta_i}{\Lambda} n - \lambda_i c_i,$$ (2.2.29)

that is known as point kinetics equations.

Step-Input Response

To clarify how the parameters β and Λ play an important role in the temporal dynamic of a nuclear reactor, let us see the example of a sudden reactivity change in a critical system (step-input response).

The former differential equation system, for a constant reactivity and in the abscence of a external source has the following solution

$$n(t) = \sum_{i=1}^{7} A_i e^{\omega_i t}$$ (2.2.30)

Consider now we only have one group of precursors, a critical system with a constant neutron population, $n(t \leq 0) = n_0$, and we make a sudden change in reactivity in $t = 0$. Therefore, $q(t) = 0$ and $\rho(t < 0) = 0$, $\rho(t \geq 0) = \rho_0$. For that problem, the following solution can be found [14]

$$n(t) \approx \frac{n_0}{\beta - \rho_0} \left[\beta \exp\left(\omega_1 t\right) - \rho_0 \exp\left(\omega_2 t\right) \right],$$ (2.2.31)

where ω_1 and ω_2 are

$$\omega_1 \approx \frac{\lambda \rho_0}{\beta - \rho_0},$$ (2.2.32)

$$\omega_2 \approx \frac{\rho_0 - \beta}{\Lambda}.$$ (2.2.33)

The parameter ω_1 is related with the delayed neutrons. If $\rho_0 < \beta$, ω_2 is negative and the second term of (2.2.31) tends to zero in time. Then, the neutron density (and the power of the reactor) is dominated by the first term, in other words, by the delayed neutrons, as we can see in figure 2.2.1. Since the delayed neutron decay constants (λ) are on the order of 0.1 s^{-1} , this will result in relatively long reactor periods (in the order of seconds or larger, depending on the

---

[2]The reactivity is an alternative to the criticality constant to measure the departure from the critical state. It is zero for a critical system, negative in a subcritical system and positive in a supercritical system. Like k, it is an adimensional quantity and it is customary to express it in parts per cent mille (pcm).

value of ρ_0), which will make the reactor controlable by insertion or extraction of control rods.

On the other hand, if $\rho_0 > \beta$, the timescale of the reactor power variation will be largely determined by Λ. Typical values for this parameter may vary between $\sim 10^{-3}$ s for thermal reactors and $\sim 10^{-8}$ s for fast reactors, thus resulting in reactor periods too short to control the reactor by means of control rods. It is beta the parameter that fixes the limit between these two regimes, hence the importance of an accurate knowledge of this parameter for reactor design.
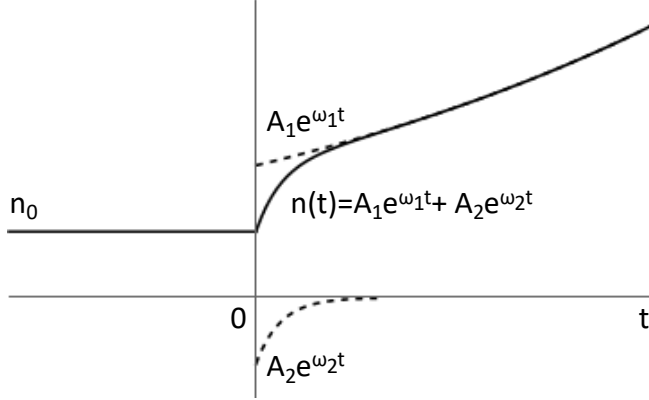

Figure 2.2.1: Neutron density as a function of time for a step input response and one group of delayed neutrons. The dashed lines are the terms of equation (2.2.31).

Effective major parameters: β_{eff} **and** Λ_{eff}

Up to now, we defined the major parameters β and Λ in a system with a single energy group and a single region. In a real system, these parameters have to be weighted by the neutron flux (both its spatial and energy distributions) and they are also weighted by the so-called adjoint flux, which can be interpreted as the number of new fissions that can be induced by a given neutron (hence also referred as "neutron importance"). For details, see for instance [15]. So, we have to define the *effective* major parameters.

Mathematically, we can define the effective delayed neutron fraction as

$$\beta_{eff} = \frac{\langle \phi^*, \hat{F}_d \phi \rangle}{\langle \phi^*, \hat{F} \phi \rangle}, \tag{2.2.34}$$

where $\hat{F}$ is the fission operator ($\hat{F} = \nu \Sigma_f$, i.e. the operator number of neutrons produced by fission), $\hat{F}_d$ is the operator number of delayed neutrons produced by fission ($\hat{F}_d = \nu_d \Sigma_f$) and ϕ^* is the adjoint flux. The brackets denote an integral over the entire space and all energies and velocities of the neutrons.

In the same way, we can define the effective neutron generation time as

$$\Lambda_{eff} = \frac{\langle \phi^*, \frac{1}{v} \phi \rangle}{\langle \phi^*, \hat{F} \phi \rangle}, \tag{2.2.35}$$

where v is the neutron speed. Λ_{eff} can be understood also as the inverse of the average neutron production probability or the average time before one neutron produces another.

16

3   S/U calculations and Reactor databases

In this chapter we will introduce the mathematical tools used for the sensitivity and uncertainty analysis and the different reactor databases we have used in this work.

3.1   Propagation of errors in nuclear data to reactor parameters: Sandwich rule and covariance matrices. The SUMMON code. Sensitivity coefficients and sensitivity profiles.

In this subsection, we are going to introduce the main concepts of uncertainty and sensitivity analysis we will use in this thesis (first order perturbation theory, sandwich rule, sensitivity coefficient, etc.), the SUMMON code and the sensitivity coefficients of the reactor parameters.

3.1.1   Uncertainty and sensitivity analysis

Sensitivity analysis allow us calculating the variation of a response of our system under changes in its input parameters and studying the importance of different nuclear data in this response. Uncertainty analysis allows us calculating the errors in our system response due to nuclear data uncertainties.

We will focus on local analysis, which accounts only for the first order contribution to the total response variation and works only in the neighbourhood of the nominal values of different parameters (input data) [16]. So, we can consider the response of the major reactor parameters (like k_{eff}[3], β_{eff} and Λ_{eff}) linear with respect to local variation in the nuclear data provide to the system that we are going to study.

Next, we will introduce the Sandwich rule, essential in uncertainty analysis, which is based in the first order perturbation theory, where the sensitivity coefficient concept will appear, fundamental idea in sensitivity analysis.

First order perturbation theory

Let us define $R = f(\alpha_1, ..., \alpha_k)$ as the response of our system and $(\alpha_1, ..., \alpha_k)$ the real values of our system input parameters that are unknown and we can write them as

$$(\alpha_1, ..., \alpha_k) = (\alpha_1^0, ..., \alpha_k^0) + (\delta\alpha_1, ..., \delta\alpha_k) = \alpha^0 + \delta\alpha, \qquad (3.1.1)$$

where α^0 are the nominal values taken as the expected values and $\delta\alpha$ their uncertainties taken as the standard deviation. We can expand the system response with a Taylor series around α^0

_____

[3]This is an usual notation for the multiplication factor.

$$R(\alpha_1, ..., \alpha_k) = R(\alpha^0) + \sum_{i_1=1}^{k} \left(\frac{\partial R}{\partial \alpha_{i_1}} \right)_{\alpha_0} \delta\alpha_{i_1} +$$

$$+ \frac{1}{2} \sum_{i_1 i_2=1}^{k} \left(\frac{\partial^2 R}{\partial\alpha_{i_1}\partial\alpha_{i_2}} \right)_{\alpha_0} \delta\alpha_{i_1}^2 \delta\alpha_{i_2}^2 + ... \qquad (3.1.2)$$

$$... + \frac{1}{n!} \sum_{i_1,...,i_n=1}^{k} \left(\frac{\partial^n R}{\partial\alpha_{i_1}...\partial\alpha_{i_n}} \right)_{\alpha_0} \delta\alpha_{i_1}^n ... \delta\alpha_{i_n}^n.$$

Therefore, assuming linearity

$$R(\alpha_1, ..., \alpha_k) = R(\alpha^0) + \sum_{i=1}^{k} \left(\frac{\partial R}{\partial \alpha_i} \right)_{\alpha_0} \delta\alpha_i = R^0 + \sum_{i=1}^{k} S_i \delta\alpha_i, \qquad (3.1.3)$$

where $R^0 = R(\alpha^0)$ and $S_i = (\partial R/\partial\alpha_i)_{\alpha_0}$.

The terms S_i are the sensitivity coefficient of R due to change in α_i. They are commonly expressed in relative terms (dimensionless):

$$S_{R,\alpha_i} = \frac{\alpha_i}{R} \frac{\partial R}{\partial \alpha_i}. \qquad (3.1.4)$$

In this work, R is the reactor parameter and α is the nuclear data (usually, the value of a cross section in a specified energy range). A set of sensitivity coefficients covering the complete energy range make up a sensitivity profile. Since the nuclear data depends on energy, we usually plot this sensitivity profiles as a function of energy, as we can see in figure 3.1.1. In the next section, we will calculate the sensitivity coefficients for the main reactor parameters (k_{eff}, β_{eff} and Λ_{eff}). With this coefficients and the covariance matrix, we will be able to obtain the variance of the response due to nuclear data errors. As we will see, when the sensitivity coefficients are calculated with Monte Carlo codes, which are based on stochastic methods, the sensitivity coefficients will have statistical errors.
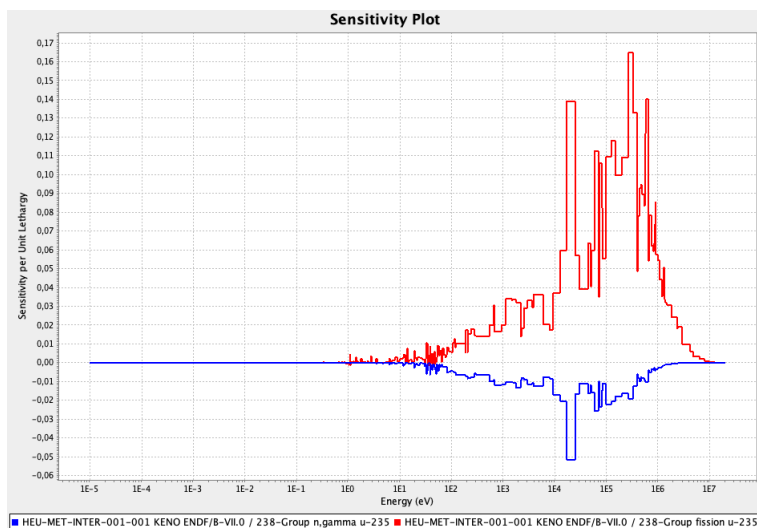

Figure 3.1.1: Sensitivity profile for fission and capture of ^{235}U in the HEU-MET-INTER-001 benchmark experiment [17].

Sandwich Rule

Using first perturbation theory, we can obtain the variance of the response due to nuclear data uncertainties

$$\sigma_R = var(R) = E[(R - E[R])^2] = E[(R - R^0)^2] =$$

$$= \int \left(\sum_{i=1}^{k} S_i \delta\alpha_i \right)^2 p(\alpha_1, ..., \alpha_k) \partial\alpha_1...\partial\alpha_k =$$

$$= \sum_{i=1}^{k} S_i^2 \int (\delta\alpha_i)^2 p(\alpha_1, ..., \alpha_k) \partial\alpha_1...\partial\alpha_k +$$

$$+ 2 \sum_{i \neq j=1}^{k} S_i S_j \int (\delta\alpha_i)(\delta\alpha_j) p(\alpha_1, ..., \alpha_k) \partial\alpha_1...\partial\alpha_k =$$

$$= \sum_{i=1}^{k} S_i^2 var(\alpha_i) + 2 \sum_{i \neq j=1}^{k} S_i S_j cov(\alpha_i, \alpha_j)) = S V_\alpha S^T$$

$$(3.1.5)$$

where V_α is the covariance matrix of the $(\alpha_1, ..., \alpha_k)$ nuclear data and p is a propability function. This equation is known as the Sandwich Rule.

Correlations may appear between the energy ranges of a given cross section (or other nuclear parameters), between different cross section of a given isotope or between different cross sections of different isotopes. Information about data uncertainties and correlations is containing in covariance matrices.

We can rewrite sandwich rule by using another two types of matrices. One with the correlation coefficients $corr(\alpha_i, \alpha_j) = cov(\alpha_i, \alpha_j)/\sqrt{var(\alpha_i)var(\alpha_j)}$ (dimensionless and with a range between -1 and 1), or with the relative covariance $rcov(\alpha_i, \alpha_j) = cov(\alpha_i, \alpha_j)/(E[\alpha_i]E[\alpha_j])$ (dimensionless).

Applying the equation (3.1.5) to the variance of the response, we obtain the variance due to statistical errors of that quantity

$$std_{\sigma_R}^2 = std_S^2 (V_\alpha S^T)^2 + (S V_\alpha)^2 std_{S^T}^2 \qquad (3.1.6)$$

To sum up, our response is always affected by two types of uncertainties. One due to statistical errors in the parameters for the use of Monte Carlo codes to calculate the response, measuring the statistical fluctuation (it can be controlled by increasing the number of particles simulated). The other due to nuclear data uncertainties (when nuclear data is the main source of input data uncertainties).
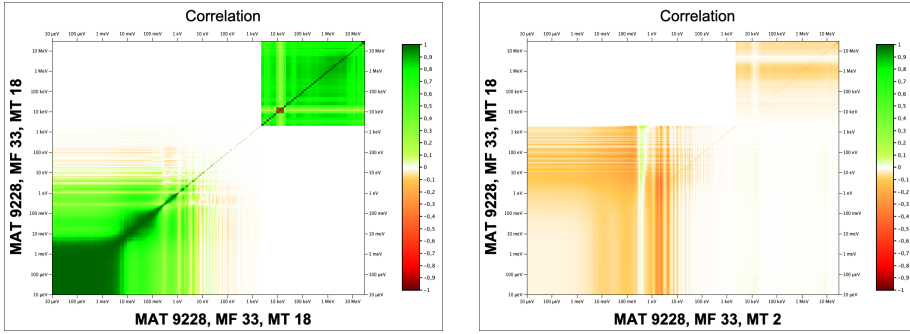
Figure 3.1.2: (a) Correlation matrix for the fission cross section of ^{235}U [10]; (b) Correlation matrix for the elastic scattering and fission cross section of ^{235}U [10].

3.1.2 The SUMMON code

Sensitivity and Uncertainty Methodology for MONte carlo codes [9] (SUMMON) is a tool to perform sensitivity and uncertainty analyses of the most relevant criticality safety parameters in a nuclear reactor (k_{eff}, β_{eff} and Λ_{eff}) and reactivity responses (i.e. reactivity differences between two reactor states or configurations). SUMMON was designed to work with sensitivity profiles calculated by any code providing that they are supplied in the SDF format [18], and covariance matrices from any nuclear data library, providing that they are in the Boxer format [19]. In this work, we have used sensitivity profiles calculated with MCNP 6.2 (KSEN card) [20] and the JEFF-3.3 library. Sensitivity profiles were provided in a 33 energy group structure [21], using covariance matrices from several libraries (JEFF-3.3, ENDF/B-VIII.0 and JENDL-4.0u).

Like we saw in the former section, assuming a linear system response (which is valid in many cases of interest), we can use local sensitivity and uncertainty analysis, which is efficient in computer time. On the contrary, global analysis accounts with high-order terms and requires large computational resources. Thus, the methodologies implemented in SUMMON are based on local analysis [9].

3.1.3 Sensitivity coefficients and sensitivity profiles

As stated above, for this work we have sensitivity profiles calculated for the criticality constant k_{eff} with the KSEN card of the code MCNP. In this section, we are going to explain how SUMMON calculate sensitivity coefficients to parameters other than k_{eff} from the sensitivity coefficients to the criticality constant k_{eff}.

Multiplication factor and reactivity sensitivity coefficients

Let us start by the simple case of calculating the sensitivity coefficient of a reactivity response (i.e. a reactivity difference between two reactor states or configurations). The reactivity for the initial state is

$$\rho_1 = 1 - \frac{1}{k_{eff,1}}, \tag{3.1.7}$$

and we perform a perturbation in the system, which lead to a new state with the following k_{eff}

20

$$\frac{1}{k_{eff,2}} = \frac{1}{k_{eff,1}} + \Delta\left(\frac{1}{k_{eff,1\to2}}\right), \tag{3.1.8}$$

$$\rho_2 = 1 - \frac{1}{k_{eff,2}}. \tag{3.1.9}$$

The change in reactivity can be written as

$$\rho_{1\to2} = \rho_2 - \rho_1 = \frac{1}{k_{eff,1}} - \frac{1}{k_{eff,2}}. \tag{3.1.10}$$

Using now the sensitivity coefficient definition (3.1.4), we get the following equation

$$S_{\rho_{1\to2},\alpha} = \frac{\alpha}{\rho_{1\to2}} \frac{\partial \rho_{1\to2}}{\partial \alpha} = \frac{\alpha}{\rho_{1\to2}}\left(\frac{\partial(1/k_{eff,1})}{\partial \alpha} - \frac{\partial(1/k_{eff,2})}{\partial \alpha}\right) =$$

$$\tag{3.1.11}$$

$$= \frac{-k_{eff,2}S_{k_{eff,1},\alpha} + k_{eff,1}S_{k_{eff,2},\alpha}}{k_{eff,2} - k_{eff,1}}.$$

where $S_{k_{eff,1},\alpha}$ and $S_{k_{eff,2},\alpha}$ are the sensitivity coefficients of $k_{eff,1}$ and $k_{eff,2}$ respectively. This sensitivity coefficient can be written as

$$S_{\rho_{1\to2},\alpha} = f(k_{eff,1}, k_{eff,2}, S_{k_{eff,1},\alpha}, S_{k_{eff,2},\alpha}), \tag{3.1.12}$$

where f can be considered a linear function of the variables in the context of the first perturbation theory ($k_{eff,1}$, $k_{eff,2}$, their sensitivity coefficients and their standard deviation are calculated by MCNP with the KSEN card). Assuming this linearity, we can evaluate the standard deviation of the sensitivity coefficient $std^2_{S_{\rho_{1\to2},\alpha}}$ using (3.1.5) but, in that case, uncertainty is due to the stochastic nature of the Monte Carlo code. This kind of propagation is performed by SUMMON. It also consider negligible the correlation between both states due to stochastic Monte Carlo calculations and, to be conservative (due to the difficulty to calculate the correlation between k_{eff} and the sensitivity coefficients), it takes full positives or negative correlations depending on the case, maximizing the standard deviation of the sensitivity coefficient [9].

Effective delayed neutron fraction sensitivity coefficient

A common way to calculate β_{eff} with Monte Carlo codes has been proposed by Bretscher [22] and is sometimes referred as the "prompt method":

$$\beta_{eff} \approx 1 - \frac{k_p}{k_{eff}}, \tag{3.1.13}$$

where k_p is the effective multiplication factor of the prompt neutrons. With the definition of sensitivity coefficient (3.1.4) and the former equation, we can obtain

$$S_{\beta_{eff},\alpha} = \frac{\alpha}{\beta_{eff}} \frac{\partial \beta_{eff}}{\partial \alpha} = \frac{\alpha}{\beta_{eff}} \frac{\partial}{\partial \alpha} \left(1 - \frac{k_p}{k_{eff}} \right) =$$

$$= \frac{\alpha}{\beta_{eff}} \left(-\frac{1}{k_{eff}} \frac{\partial k_p}{\partial \alpha} + \frac{k_p}{k_{eff}^2} \frac{\partial k_{eff}}{\partial \alpha} \right) =$$

$$= \frac{k_p}{k_{eff} - k_p} \left(\frac{\alpha}{k_{eff}} \frac{\partial k_{eff}}{\partial \alpha} - \frac{\alpha}{k_p} \frac{\partial k_p}{\partial \alpha} \right) =$$

$$= \frac{k_p}{k_{eff} - k_p} \left(S_{k_{eff},\alpha} - S_{k_p,\alpha} \right),$$

$$(3.1.14)$$

where $S_{k_{eff},\alpha}$ and $S_{k_p,\alpha}$ are the sensitivity coefficients of k_{eff} and k_p respectively (all of them and their standard deviation are obtained by MCNP with the KSEN card). The k_p parameter can be calculated with Monte Carlo codes by switching off the sampling of delayed neutrons, in MCNP this is achieved with the TOTNU card [20]. The statistical (Monte Carlo) standard deviation of β_{eff} and $S_{\beta_{eff},\alpha}$ are also obtained in SUMMON using error propagation as explained above. Once again, SUMMON assumes negligible correlations between the two states (the prompt neutrons state and the normal) and full possitives or negatives correlations depending on the case.

To reduce statistical errors, we can use a variation of prompt method which consider a new state where we introduce a scaling factor a in order to adjust the perturbation from the reference state (Chiba's approximation, that is a perturbative method) [23]. Performing analogous calculation, we obtain

$$\beta_{eff} \approx \frac{1}{a} \left(\frac{\bar{k}_{eff}}{k_{eff}} - 1 \right), \qquad (3.1.15)$$

$$S_{\beta_{eff},\alpha} = \frac{\alpha}{\beta_{eff}} \frac{\partial \beta_{eff}}{\partial \alpha} = \frac{\bar{k}_{eff}}{k_{eff} - \bar{k}_{eff}} \left(S_{k_{eff},\alpha} - S_{\bar{k}_{eff},\alpha} \right) \qquad (3.1.16)$$

where $\bar{k}_{eff}$ and $S_{\bar{k}_{eff},\alpha}$ are the multiplication factor and its sensitivity coefficient of the new state, calculated along with their standard deviation, using a nuclear data library in which $\bar{\nu}_d$ is multiplied by $(a + 1)$. In the particular case $a = -1$, equation (3.1.15) is the Bretscher's method equation (3.1.13). Like in the previous case, we can evaluate the standard deviation of β_{eff} and $S_{\beta_{eff},\alpha}$ with SUMMON.

Chiba's method reduce the statistical uncertainty of β_{eff} and $S_{\beta_{eff},\alpha}$ compared with the prompt method [24]. The statistical error of both, the delayed neutron fraction and the sensitivity profile are proportional to $\sim 1/a$. A disadvantage is that larger value of a introduces systematic errors in the calculations and that Chiba's method requires modified nuclear data files. Both method are available in SUMMON, but Chiba's method can be used only if the Monte Carlo code we are employing supports the modified nuclear data files.

3.2 Reactor databases (ICSBEP, IRPhE).

In this section, we are going to talk about the definition of integral experiments and its relevance in nuclear research and the main databases used to store the data of these experiments.

3.2.1 Integral experiments and zero power reactors

Zero power reactors (or mock-ups reactors) are experimental reactor with very low power, so that they do not have changes in temperature during relevant operation and they do not need a coolant. They consist in very simplified reactor models whose purpose is to measure the main reactor parameters in experiments, which can be used later to validate neutronic calculations. These experiments are known as integral experiments because the parameters being measured depend on many cross sections of many isotopes in all the energy range (on the other hand, differential experiments, which are conducted in accelerator facilities, try to measure cross sections for each isotope and energy range). For a historical introduction to this kind of reactors and some examples see [25].

3.2.2 Reactor databases

The data obtained in integral experiments, in particular, those conducted with zero power reactors, are stored in integral experiment databases. In this thesis, we will focus on two of them, ICSBEP [26] and IRPhE [27].

ICSBEP

ICSBEP (International Criticality Safety Benchmark Evaluation Project) is a data base whose purpose is to compile critical and subcritical benchmark experiment data into a standardised format that allows to validate calculation tools and cross-section libraries. In 1992, the CSBEP was created by the US Department of Energy, in the National Engineering and Environmental Laboratory (INEEL). In 1995, it was renamed as ICSBEP when it was transferred to the OECD-NEA (Nuclear Energy Agency).

ICSBEP database is focussed in the k_{eff}, to search experimental results for other parameters of ICSBEP experiments we have to go to bibliography. ICSBEP is not a public database, but a set of its data is available through the DICE tool [17].

The experiments are classified by fissile fuel (highly enriched uranium, mixed enrichment uranium, ...), physical form of the fissile material (metal, compound, ...) and neutron energy range where the majority of the fissions occur (fast, thermal, ...). For that reason, reactors are labelled with a specific nomenclature: [Fuel]-[Physical form of fuel]-[neutron energy spectrum]-[case] (for example, HEU-MET-INTER-001 is high enriched uranium in metal form with intermediate energy spectrum, case 1).

Eighteen experiments have been selected from ICSBEP. There are twelve ^{235}U systems, one with intermediate neutron energy spectrum, nine with fast neutron energy spectrum and two with thermal neutron energy spectrum. There is one ^{233}U system with fast neutron energy spectrum. There are five ^{239}Pu systems, two

with intermediate neutron energy spectrum and three with fast neutron energy spectrum.

IRPhE

IRPhE (International Handbook of Evaluated Reactor Physics Benchmark Experiments) is a database which contains experimental reactor physics data obtained at several nuclear facilities around the world. It is also maintained by the NEA. As ICSBEP, this is not a public reactor database, but a set of its data is available through the IDAT tool [28].

In ICSBEP, with exceptions, we only find k_{eff} but, in IRPhE we can also find reaction rate distribution, spectral characteristics, isotopic composition, reactivity coefficients, etc. Data of β_{eff} is only included for some reactors. The information is organised by reactor type and use a similar format to ICSBEP with subsections for each measurement type. From IRPhE, we have selected two reactors: SNEAK-7A and SNEAK-7B (^{239}Pu systems with fast neutron spectrum)

Other sources

The reactors MASURCA_R2, MASURCA_ZONA2, FCA-XIX-1, 2 and 3 have been selected from an international program of benchmark experiments developed at CEA (France) and JEARI (Japan) to improve the accuracy of prediction of β_{eff} [29].

4 Work methodology

In this section, we will introduce the experiments we have studied and explain the methodology we have used in the thesis to achieve our final results.

4.1 Benchmark experiments

In this subsection, we will perform a brief description of the benchmark experiments used in this work from different databases.

4.1.1 ^{235}U systems

Table 4.1.1: Benchmark experiments of ^{235}U systems data from [17] and [29]. wt%.

Database name/ β_{eff} Ref.	Reactor name & lab.	Comments
HEU-MET-INTER -001/ [30], [31]	The Uranium/Iron Benchmark Assembly ANL (USA) 1980s	Highly enriched metallic uranium (93.18% ^{235}U) cylinder reflected by stainless steel (Fe, Cr, Ni)
IEU-MET-FAST -010/ [32], [30]	U9 Benchmark Assembly ANL (USA) 1981	Intermediate enriched metallic uranium (8.88% ^{235}U) cylinder reflected by depleted uranium
IEU-MET-FAST -020/ [26]	The FR0 Series 1 Studsvik (Sweden) 1964	Intermediate enriched metallic uranium (20.05% ^{235}U) cylinder reflected by copper
IEU-MET-FAST -021/ [26]	The FR0 Series 4 Studvik (Sweden) 1965	Intermediate enriched metallic uranium (20.05% ^{235}U) cylinder reflected by natural uranium
IEU-MET-FAST -022/ [26]	The FR0 Experiments Studvik (Sweden) 1965	Intermediate enriched metallic uranium (20.05% ^{235}U) cylinder reflected by copper
LEU-COMP- THERM-006/ [33], [31], [30]	JAEA (Japan) 1963-75	Low enriched uranium oxide (2.60% ^{235}U) array reflected and moderated by light water
LEU-COMP- THERM-067/ [26]	IPEN/MB-01 IPEN (China) 2014	Low enriched uranium oxide (4.35% ^{235}U) configuration reflected and moderated by light water
HEU-MET-FAST -001/ [30], [31]	Godiva LANL (USA) 1950s	Unreflected, highly enriched metallic uranium (93.71% ^{235}U) sphere
HEU-MET-FAST -028/ [30], [31], [34]	Topsy LANL (USA) 1964-66	Highly enriched metallic uranium (93.24% ^{235}U) sphere reflected by natural uranium

Table 4.1.2: Benchmark experiments of ^{235}U systems data from [17] and [29]. wt%.

Database name/ β_{eff} Ref.	Reactor name & lab.	Comments
IEU-MET-FAST -007/ [30], [31]	Big Ten LANL (USA) 1971-80	Intermediate enriched metallic uranium (10.06% ^{235}U) cylinder reflected by depleted uranium
FCA-XIX-1/ [35], [29], [30]	FCA JAERI (Japan) 1995-98	^{235}U core surrounded by an inner blanket of depleted uranium oxide and sodium and an outer blanket of depleted uranium metal
MASURCA_R2/ [29], [30]	MASURCA CEA (France) 1993-94	^{235}U core surrounded by a blanket of 50-50 $UO_2 - Na$ mixture blanket
HEU-MET-FAST -062/ [36]	Coral-I CIEMAT (Spain) 1968	Highly enriched metallic uranium (89.74% ^{235}U) cylinder reflected by natural uranium
HEU-MET-FAST -100/ [26], [27]	Orsphere ORNL (USA) 1972-75	Unreflected, highly enriched metallic uranium (93.20%) sphere

4.1.2 ^{239}Pu systems

Table 4.1.3: Benchmark experiments of ^{239}Pu systems data from [17] and [29]. wt%.

Database name/ β_{eff} Ref.	Reactor name & lab.	Comments
MIX-COMP-FAST -005/ [32], [30]	ZPR-9 ANL (USA) 1976-77	Mixed (Pu,U)-Carbide fuel with metallic plutonium (87.22% ^{239}Pu and 0.21% ^{235}U) cylinder reflected by uranium carbide and stainless steel (Fe, Cr, Ni)
PU-MET-INTER -002/ [32]	ZPR-6 ANL (USA) 1981-82	Metallic plutonium (95.31% ^{239}Pu) cylinder moderated by graphite and reflected by iron and stainless steel (Fe, Cr, Ni)
PU-MET-INTER -004/ [37]	ZPR-3 ANL-W (USA) 1969	Metallic plutonium (95.47% ^{239} Pu) cylinder moderated by graphite and reflected by lead
PU-MET-FAST -001/ [31], [30]	LANL (USA) 1954-55	Metallic plutonium (95.18% ^{239}Pu) sphere
PU-MET-FAST -006/ [31], [30], [34]	Flattop LANL (USA) 1964-66	Metallic plutonium (94.84% ^{239}Pu) sphere reflected by natural uranium

Table 4.1.4: Benchmark experiments of ^{239}Pu systems data from [28] and [29]. wt%.

Database name/ β_{eff} Ref.	Reactor name & lab.	Comments
FCA-XIX-2/ [35], [29], [30]	FCA JAERI (Japan) 1995-98	^{239}Pu and natural uranium core surrounded by an inner blanket of depleted uranium oxide and sodium and an outer blanket of depleted uranium metal
FCA-XIX-3/ [35], [29], [30]	FCA JAERI (Japan) 1995-98	^{239}Pu core surrounded by an inner blanket of depleted uranium oxide and sodium and an outer blanket of depleted uranium metal
SNEAK-LMFR-EXP-001/ [30]	SNEAK-7A KIT (Germany) 1970-71	$PuO_2 - UO_2$ fast critical assembly reflected by depleted UO_2 with some graphite moderator
SNEAK-LMFR-EXP-001/ [30]	SNEAK-7B KIT (Germany) 1970-71	$PuO_2 - UO_2$ fast critical assembly reflected by depleted UO_2
MASURCA _ZONA2/ [29], [30]	MASURCA Zona2 CEA (France) 1993-94	$PuO_2 - UO_2$ fast critical assembly reflected by depleted UO_2 with sodium to simulate coolant

4.1.3 ^{233}U systems

Table 4.1.5: Benchmark experiments of ^{233}U systems data from [17]. wt%.

Database name/ β_{eff} Ref.	Reactor name & lab.	Comments
U233-MET-FAST 006/ [31], [30] [34]	Flattop LANL (USA) 1964	Highly enriched metallic uranium (98.13% ^{233}U) reflected by natural uranium

4.2 Simulation and analysis procedure

In this work, twenty five MNCP inputs mainly from ICSBEP and IRPhE databases have been modified to adapt them for sensitivity calculations with the MCNP code (v6.2) and the JEFF-3.3 library. Modifications consisted mainly in modifying the isotopic compositions, implementing the 33-group structure in the KSEN card described in subsection 3.1.2 and other required modifications to apply Bretscher's and Chiba's methodologies for β_{eff} calculations. Once MCNP outputs were available, sensitivity data (senstivity profiles and their statistical uncertainty) were converted into the SDF format described in subsection 3.1.2 in order to work with the SUMMON code. Version 2.2 of SUMMON has been used in this work. With SUMMON we have evaluated the uncertainty due to nuclear data and its statistical error with three covariance matrices from different nuclear data libraries (JEFF-3.3, JENDL-4.0u and ENDF/B-VIII.0). Notice that covariance matrices from all three libraries were combined with sensitivity profiles calculated with JEFF-3.3; this has been done in this way because sensitivity profiles require long calculation

times and usually change little between libraries, while on the other hand the use of a covariance matrix from one library or another may have a large impact in the results.

5 S/U analysis of the results

In this section, results of S/U analyses for the k_{eff} and β_{eff} will be presented. They have been performed using the SUMMON code, sensitivity profiles calculated with MCNP 6.2 and the JEFF-3.3 library, and covariance matrices from the JEFF-3.3, ENDF/B-VIII.0 and JENDL-4.0u libraries. This section is divided in four parts. In the first one (subsection 5.1) we will present the general results obtained for k_{eff} and β_{eff}, in the last case with both Bretscher's and Chiba's methodologies. Then (subsection 5.2) we will present an analysis of the systematic errors introduced in the calculation of β_{eff} with Chiba's methodology. In subsection 5.3 we will present an analysis of the statistical (Monte Carlo) errors in the results. Finally, in subsection 5.4 we will discuss the most relevant reactions contributing to the uncertainty and the differences between libraries.

Given the huge amount of data produced in this work, only the most relevant results are presented here. Full results are available in [38].

5.1 Uncertainty in reactor parameters

In this subsection, we will analyze the different values of the reactor parameters and their uncertainties, both statistical and due to nuclear data.

5.1.1 Effective multiplication factor k_{eff}

Let us start with the multiplication factor k_{eff}. Observing figure 5.1.1, we can observe that the uncertainty due to nuclear data is between 0.5% and 2% (between 500 and 2000 pcm), being FCA-XIX-2 with ENDFB the reactor with the lower uncertainty (%) and IEU-MET-FAST-010 with JEFF the one with the larger uncertainty (%). In general, it seems that the relative uncertainty due to nuclear data is larger for the uranium systems than for plutonium systems (observing data for the three libraries). Looking at tables for k_{eff} in appendix A, we can observe that statistical errors of k_{eff} are very similar for all the reactors, between 0.001% and 0.004% (between 1 and 4 pcm) and are smaller than the uncertainties due to nuclear data. Hence, they are not visible in figure 5.1.2. We have not taken into account these statistical errors in error bars of figure 5.1.3 due to their small contribution.

It is worth remarking that the relative large values of the uncertainty due to nuclear data (~ 1000 pcm) are a major factor to be taken into account to determine the precision requirements of Monte Carlo calculations. I.e. it may make little sense to calculate a k_{eff} with 10 pcm statistical precision if the uncertainty due to nuclear data is 100 times larger. In this way, uncertainty calculations can be a powerful tool to optimize computational resources (for this work, all k_{eff} were obtained with a very high precision because this was required for β_{eff} calculations, as it will be shown later).

In k_{eff} tables in appendix A, we find that the statistical uncertainties of the uncertainties due to nuclear data are usually between $10^{-4}\%$ and $10^{-2}\%$ (between 0.1 and 10 pcm) and they are not visible in 5.1.1. This statistical uncertainty in the uncertainty due to nuclear data comes from the statistical uncertainty in the sensitivity profiles when they are calculated with a Monte Carlo code. In

figure 5.1.4, we can see some examples of sensitivity profiles for the multiplication factor for the MIX-COMP-FAST-005 case. We can observe that these profiles, that belong to two of the major contributors to the k_{eff} uncertainty due to nuclear data in MIX-COMP-FAST-005 ($\bar{\nu}_p$ and radiative capture cross section), have small statistical uncertainties (compare with the sensitivity profiles in figure 5.2.3, which were affected by large statistical uncertainties), that are the source of statistical error of the uncertainty due to nuclear data.

Looking at figure 5.1.2 along with figure 5.1.3, we can observe that both the experimental values and the simulation results are compatible among them within the error bars, at least, for one of the libraries in each case [4]. In general, we can observe that JEFF produces the largest nuclear data related errors and JENDL and ENDFB switch their positions depending on the case and, usually, nuclear data uncertainties are larger than the experimental ones. We will take a better look of the differences between libraries in subsection 5.4.
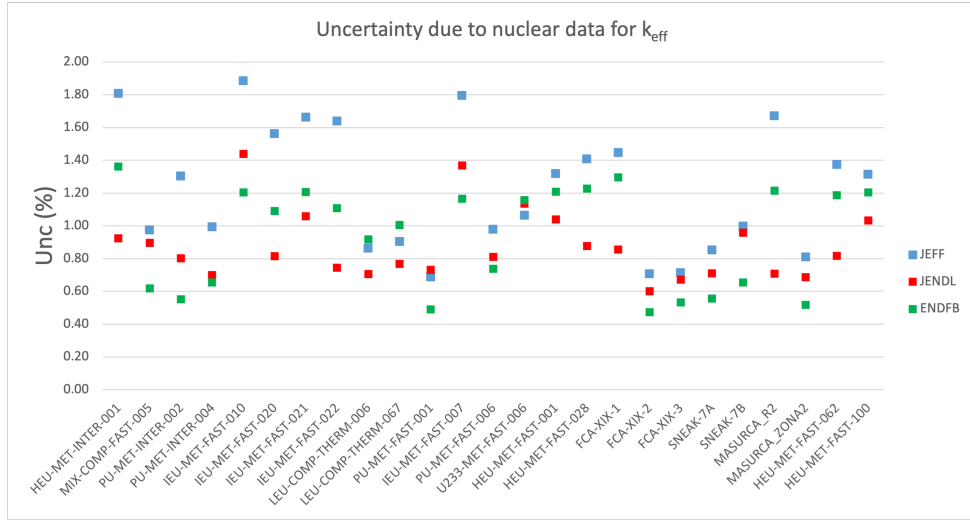

Figure 5.1.1: Uncertainties due to nuclear data (%) for k_{eff}.
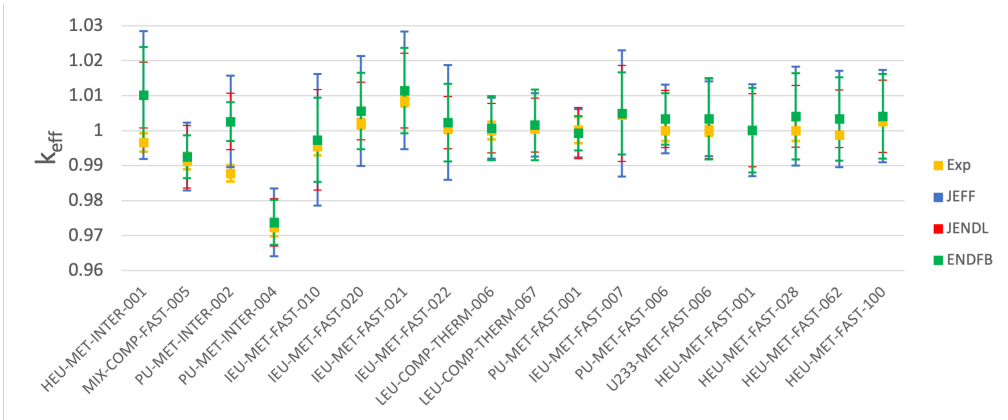
Figure 5.1.2: Experimental and calculated (MCNP) effective multiplication factor of the Benchmark reactors.

---

[4]FCA-XIX-1, FCA-XIX-2, FCA-XIX-3, SNEAK-7A, SNEAK-7B do not have experimental data of the k_{eff} because they are benchmarks specially designed for the measurement of β_{eff}.
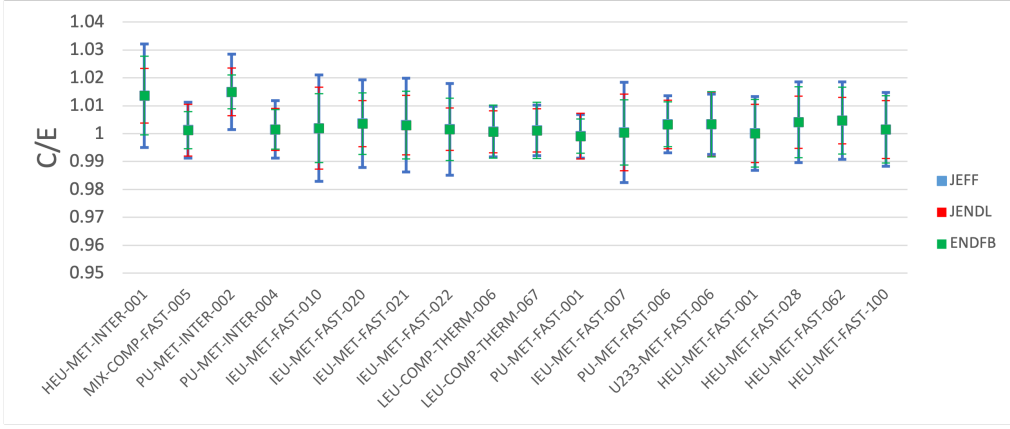
Figure 5.1.3: Calculated vs. experimental ratio for the effective multiplication factor.

(a) SP for the k_{eff} due to $\bar{\nu}_p$.

(b) SP for the k_{eff} due to (n,γ) cross section.
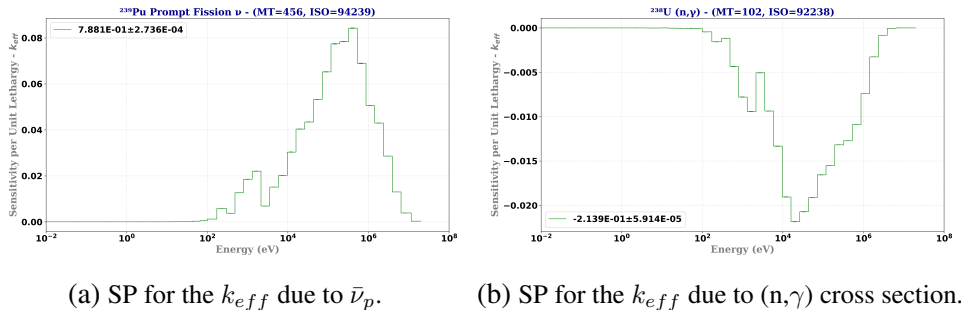
Figure 5.1.4: Examples of sensitivity profiles for k_{eff} for the MIX-COMP-FAST-005 reactor.

5.1.2 Bretscher's method β_{eff}

Now, let us see our results for the delayed neutron fraction. We start by analyzing the Bretscher's method results. Observing β_{eff} tables in appendix A and figure 5.1.5, we can see that Monte Carlo statistical errors are between 0.2% and 1.2% (between 1.4 and 4.4 pcm), but in general are lower than uncertainty due to nuclear data, that is between 0.6%, PU-MET-FAST-001 with ENDFB, and 12%, PU-MET-INTER-002 with JENDL (between 1.14 and 34.7 pcm). With respect to the statistical error of the uncertainties due to nuclear data, we have values between 0.007% and 3.6% (between 0.1 and 1.2 pcm), not negligible as we can see in figure 5.1.5 (due to larger statistical uncertainties in sensitivity profiles for Bretscher's method, as we see in subsection 5.2). In JEFF, there are some reactors where the order or magnitude of the statistical and nuclear data uncertainties of the parameter are of the same order. The same thing happens with some ^{239}Pu systems in ENDFB (for PU-MET-FAST-001, the statistical uncertainty exceeds the one due to nuclear data).

It can be noted that the lowest relative nuclear data uncertainties are usually obtained with the JEFF-3.3 library. This is due to the fact that the most relevant data contributing to the uncertainty in β_{eff} is $\bar{\nu}_d$, and the JEFF-3.3 only contains covariance information for this reaction for the case of ^{233}U (U233-MET-FAST-006). JENDL-4.0u for its part contains covariance information for $\bar{\nu}_d$ for ^{235}U and

^{239}Pu and ENDF/B-VIII.0 only for the ^{235}U. We will analyze this fact further in section 5.4.

In the figures 5.1.6 and 5.1.7 we have represented the β_{eff} along with the uncertainty due to nuclear data for JENDL. For JENDL, statistical uncertainties are usually an order of magnitude lower than uncertainty due to nuclear data, so they are not visible in the these figures and their contributions to the error has not been included in figure 5.1.8. Since the values of β (not effective, i.e the mean delayed neutron fraction of the isotopes not weighted by the flux or the neutron importance, see 2.2.3) are much larger for ^{235}U sytems than for ^{239}Pu or ^{233}U systems, they are presented in different figures. Regarding on ^{235}U cores in figure 5.1.6, we can observe that β_{eff} ranges between 650 pcm and 800 pcm, and, on the other cases in figure 5.1.7, the range is widely open and is between 200 pcm and 450 pcm (in this case, the wide range makes our study more difficult on the error bars, so it is convenient to combine the information in the figures 5.1.7 and 5.1.8, where C/E values are shown).

The uncertainty in the calculated results due to nuclear data are in general larger than in the experimental measurement, except for IEU-MET-FAST-020, 021, 022, SNEAK-7A and 7B, where experimental errors are much more larger than nuclear data uncertainties. Observing figures 5.1.6, 5.1.7 and 5.1.8 we can check that the calculated results are compatible with the experimental values, taking into account the uncertainty due to nuclear data.
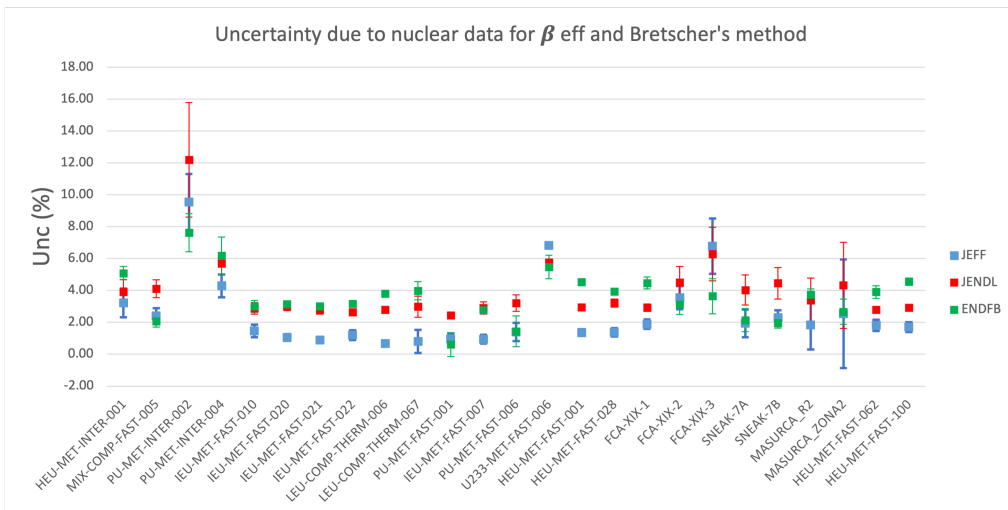
Figure 5.1.5: Uncertainties due to nuclear data (%) for β_{eff} calculated with Brestcher's method.
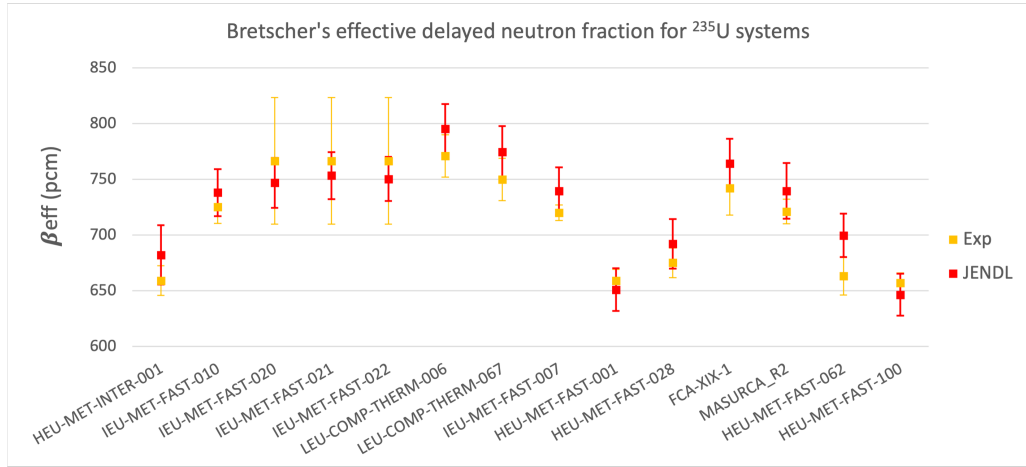
Figure 5.1.6: Experimental and evaluated with Bretscher's method effective delayed neutron fraction of the Benchmark reactors with ^{235}U.
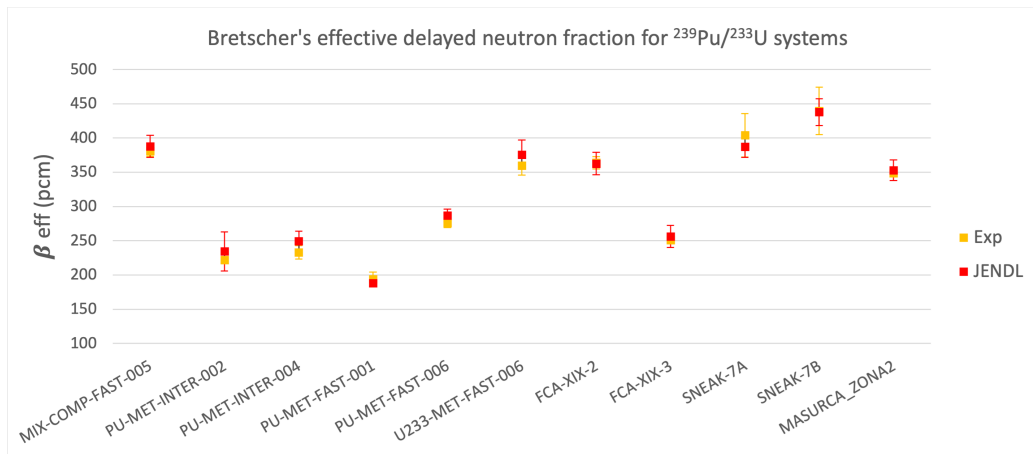
Figure 5.1.7: Experimental and evaluated with Bretscher's method effective delayed neutron fraction of the Benchmark reactors with ^{239}Pu. A ^{233}U system has also been included (U233-MET-FAST-006).
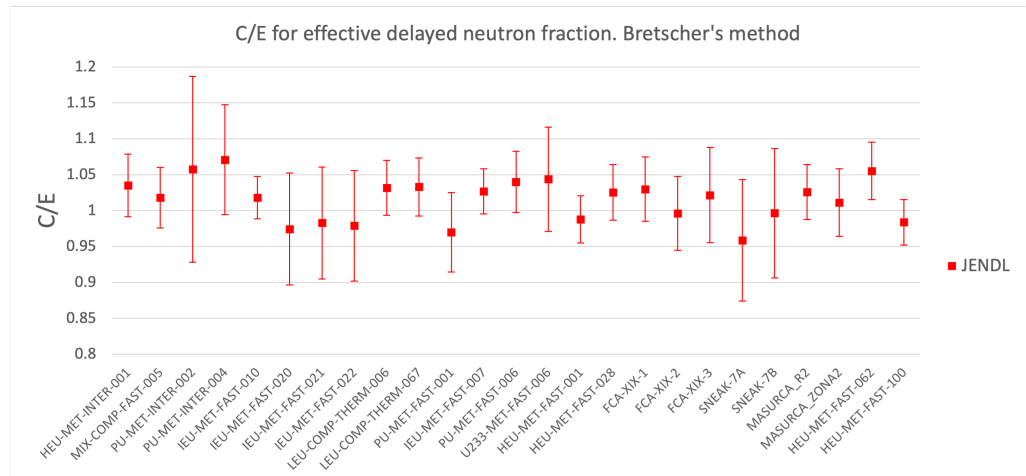
Figure 5.1.8: Calculated with Bretscher's method and experimental ratio for effective delayed neutron fraction.

5.1.3 Chiba's method β_{eff}

Regarding the β_{eff} tables of appendix A, we can observe two remarkable results in Chiba's method, in comparison with Bretscher's method. First, the statistical errors of the parameter are between 0.01% and 0.09% (between 0.1 and 0.3 pcm), so with a perturbation of $a = 20$ we have achieved an improvement in one or two order of magnitudes for the Monte Carlo statistical error of the delayed neutron fraction. For the case of the statistical error of the uncertainty due to nuclear data, the improvement reaches up to three orders of magnitude. Indeed, for Chiba's method is between 0.001% and 0.2% (between 0.004 and 0.7 pcm).

In figure 5.1.9, we observe that the uncertainties due to nuclear data are between 0.6%, LEU-COMP-THERM-067 with JEFF and 6.6% U233-MET-FAST-006 with JEFF, (between 1.15 and 32.8 pcm). There is not a clear separation between the relative uncertainties due to nuclear data of ^{235}U and plutonium systems, with the largest one for the ^{233}U system. For ^{239}Pu systems with Chiba's method, the biggest relative uncertainties due to nuclear data are clearly for JENDL, for ^{235}U systems are for ENDFB and for ^{233}U system is for JEFF. This fact will be later discussed in subsection 5.4.

Looking at the results of both methods in β_{eff} tables, it is observed that the uncertainty due to nuclear data for Chiba's method is always approximately equal or lower than the one obtained with Brestcher's method. This effect will be explained in the following subsection 5.2.

Let us take a look on figures 5.1.10, 5.1.11 and 5.1.12 . The values shown here correspond to β_{eff} obtained with Chiba's method with a perturbation of $a = 20$ for ^{235}U, ^{233}U/^{239}Pu systems and C/E, respectively. The error bars size is due to uncertainties propagated from nuclear data (statistical uncertainties will not be visible in figure 5.1.10 and 5.1.11 and their contributions to the error have not been included in figure 5.1.12). We can observe the same clear separation between β_{eff} values for ^{235}U systems and ^{235}U/^{239}Pu than we saw for Bretscher's method. In spite of the use of a large perturbation for Chiba's method, we can observe compatible results between Chiba's method evaluated delayed fraction and the experimental values. To have a better understanding of our results, in next section, we will analyze the impact of the perturbation (parameter a) of Chiba's method in the results of β_{eff} calculated with this method.
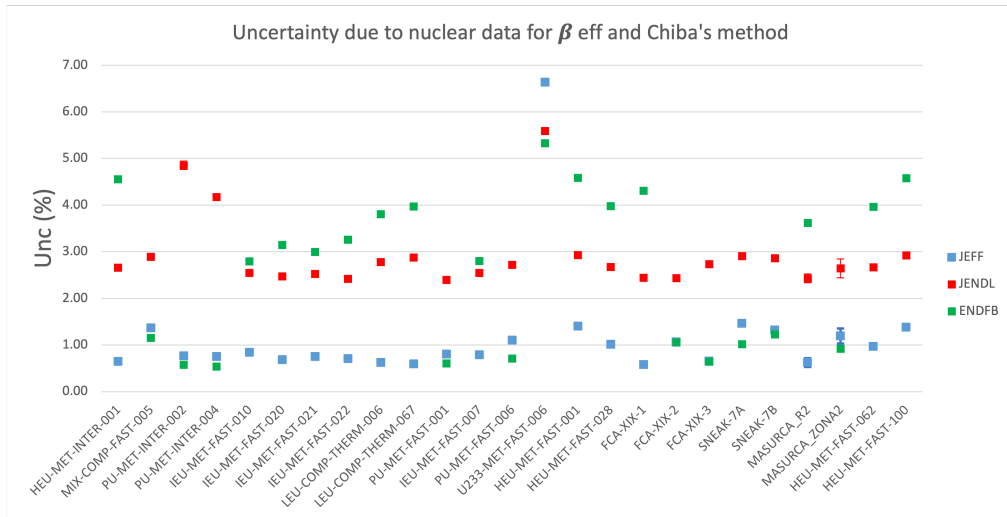
Figure 5.1.9: Uncertainties due to nuclear data (%) for β_{eff} calculated with Chiba's method.
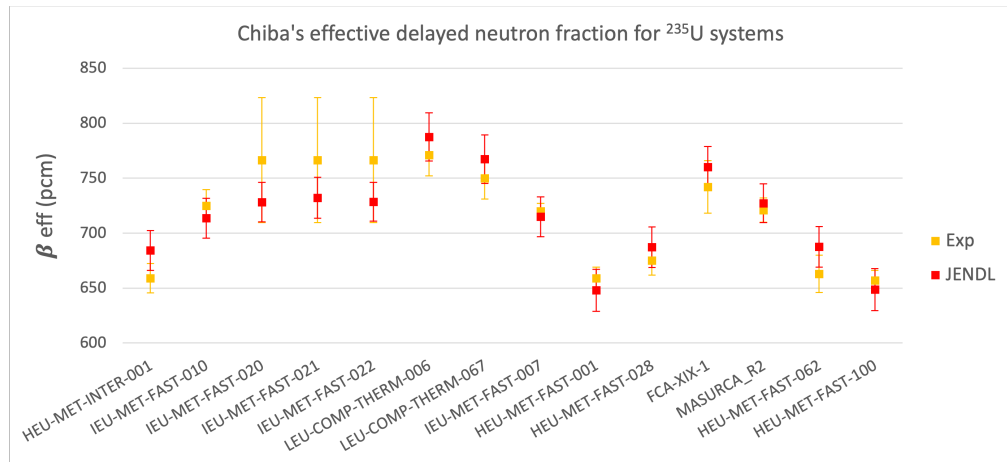

Figure 5.1.10: Experimental and evaluated with Chiba's method effective delayed neutron fraction of the Benchmark reactors with with ^{235}U.
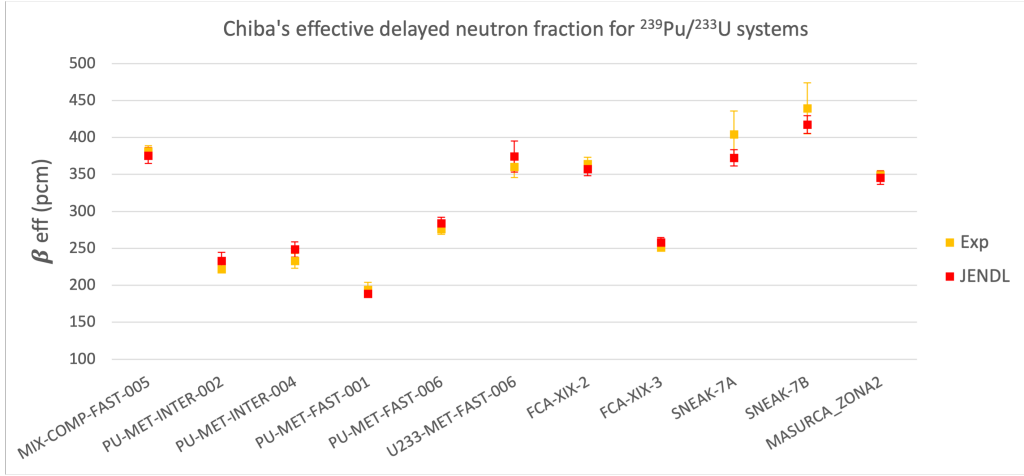
Figure 5.1.11: Experimental and evaluated with Chiba's method effective delayed neutron fraction of the Benchmark reactors with ^{239}Pu. A ^{233}U system has also been included (U233-MET-FAST-006).
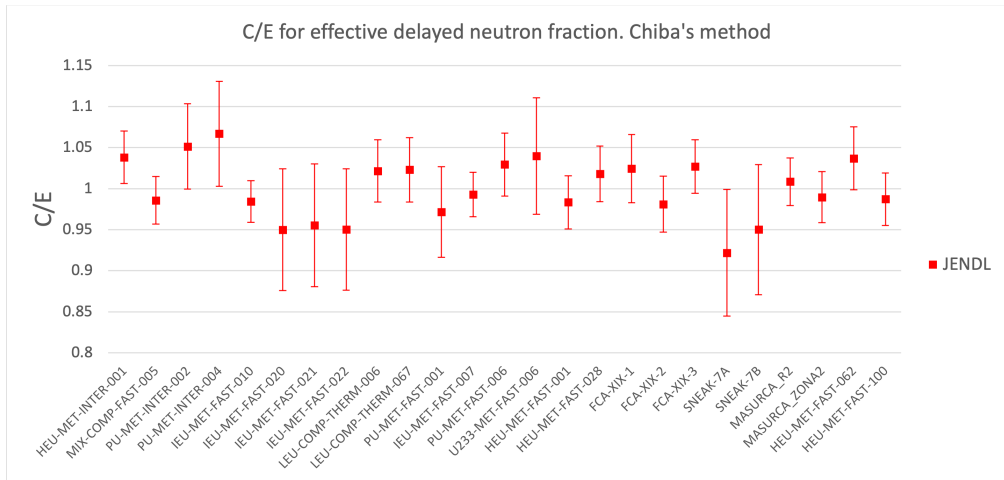

Figure 5.1.12: Calculated with Chiba's method and experimental ratio for effective delayed neutron fraction.

5.2   Systematic errors in Chiba's method

A major issue with Bretscher's method is that the delayed neutron fraction is calculated as a small difference between two similar numbers, see equation (3.1.13), which can result in large statistical error in β_{eff} and its sensitivity profiles. For that reason, in Chiba's method β_{eff} is calculated with equation (3.1.15) (in the particular case of $a = -1$, it is the Bretscher's method equation). As stated in section 3.1.3, the statistical error of both, the delayed neutron fraction and the sensitivity profile are proportional to $\sim 1/a$. Hence, a larger value of a reduces the statistical uncertainty in β_{eff} results. On the other hand, a larger value of a introduces systematic errors in the calculations.

In this subsection, we are going to analyze the results that we have obtained by varying the Chiba's method perturbation parameter for each reactor. For reasons we will explain in section 5.4, in this analysis we only take into account

JENDL library. This analysis has been performed with four reactors: HEU-MET-INTER-001, MIX-COMP-FAST-005, IEU-MET-FAST-010 and IEU-MET-FAST-007. Let us start with the study of the change in the value of β_{eff} with the a parameter.

In figures 5.2.1 and 5.2.2, we can observe the β_{eff} calculated with different values of Chiba's a parameter, the Bretscher value and the experimental result for the cases HEU-MET-INTER-001 and MIX-COMP-FAST-005. The error bars represent the experimental uncertainty, in the case of the experimental data, and the uncertainty due to nuclear data for the calculated results. In both cases, there is a very clear tendency of the value of β_{eff} with the increasing value of a. It is easy to see that this tendency is increasing in the case of HEU-MET-INTER-001 and decreasing in the case of MIX-COMP-FAST-005. As the perturbation increases and the difference between original and perturbed system is larger, the difference in β_{eff} between the two methods increases. In any case, both Bretscher's and Chiba's results (with all three values) are compatible, within errors, with the experimental results, so the value $a = 20$ for the perturbation do not seem a bad choice to estimate the delayed neutron fraction with these four benchmark reactors (for the other reactors that are not present in this subsection, Chiba's method is always used with $a = 20$).
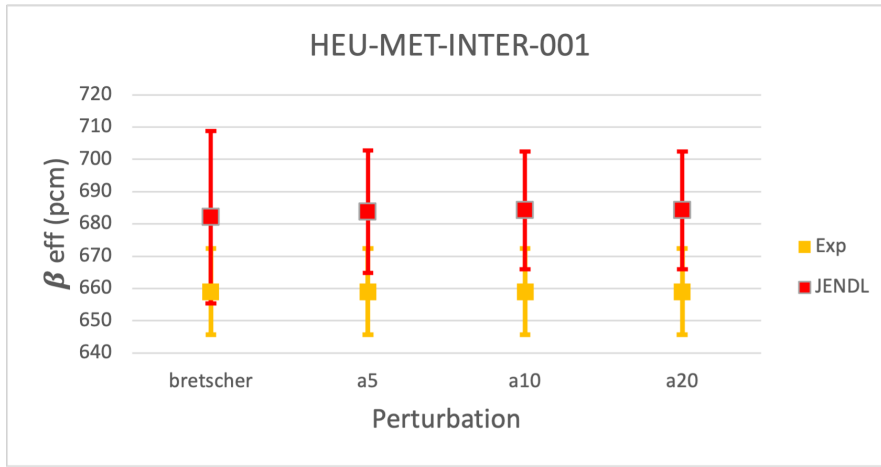
Figure 5.2.1: Experimental and Chiba's method β_{eff} for different values of the perturbation.
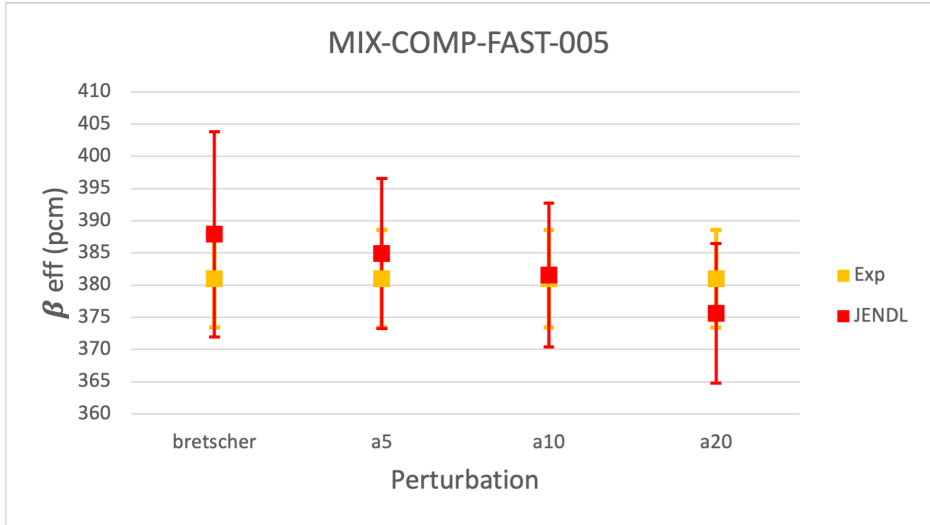
Figure 5.2.2: Experimental and Chiba's method β_{eff} for different values of the perturbation.

Now, let us take a look at the uncertainties due to nuclear data and their statistical errors. Two major results are remarkable. First, as can be expected from the own nature of Chiba's method, the statistical errors of uncertainties due to nuclear data get lower with increasing a and are lower than the ones for Bretscher's method. The second is that due to larger statistical errors in Bretscher's method, it is possible that many irrelevant reactions can show "falsely" large contributions to nuclear data uncertainty (and large sensitivity profiles), which cause an overestimation of this uncertainty. Hence, the higher statistical accuracy of Chiba's method should reduce the influence of those reactions and give us a lower value of the total uncertainty due to nuclear data [24].

In the tables 5.2.1 and 5.2.2 we can observe the different uncertainties for each reactor. We can observe a steep fall in the uncertainty due to nuclear data and the different statistical errors between Bretscher's method and Chiba's method with $a = 5$ and smaller differences between different values of a for MIX-COMP-FAST-005 and HEU-MET-INTER-001 [5].

Previously, we have said that reducing statistical error helps us to distinguish the real relevant reactions from the ones that are relevant only in Bretscher's method. So now, we are going to study the influence in the most relevant reactions of the Chiba's parameter a and the difference with Bretscher's method.

---

[5]In general, for all the libraries and in all the reactors we observe this trend. Which a small exception in the IEU-MET-FAST-010,-007 reactors with ENDFB, where a minimum is achieved for $a = 10$ and $a = 5$, respectively, and there is a tiny rise for the subsequent a. These results can be observed in [38], with the rest of the results for the Chiba analysis.

Table 5.2.1: Experimental and evaluated delayed neutron fraction of MIX-COMP-FAST-005 obtained for different cases. Uncertainty for the JENDL-4.0u library. (*) Experimental uncertainty

Case	MIX-COMP-FAST-005	
	$\beta_{eff}\pm$Stat. Unc. (pcm)	Unc. due to Data $\pm$ Stat. Unc. (pcm)
Experimental	381 ± 2*	-
Brestcher	387.9 ± 1.4	15.9 ± 2.2
$a = 5$	384.9 ± 0.3	11.6 ± 0.3
$a = 10$	381.60 ± 0.20	11.16 ± 0.14
$a = 20$	375.60 ± 0.10	10.86 ± 0.07

Table 5.2.2: Experimental and evaluated delayed neutron fraction of HEU-MET-INTER-001 obtained for different cases. Uncertainty for the JENDL-4.0u library. (*) Experimental uncertainty

Case	HEU-MET-INTER-001	
	$\beta_{eff}\pm$Stat. Unc. (pcm)	Unc. due to Data $\pm$ Stat. Unc. (pcm)
Experimental	659 ± 13.34*	-
Brestcher	682.1 ± 2.8	27 ± 5
$a = 5$	683.8 ± 0.6	19.0 ± 0.5
$a = 10$	684.2 ± 0.3	18.30 ± 0.10
$a = 20$	684.2 ± 0.1	18.22 ± 0.04

In tables 5.2.3 and 5.2.4, we will consider only the most relevant reactions contributing to the uncertainty, defined as those that explain at least 85% of the uncertainty. The gaps mean that a specific reaction has a low contribution and is not needed to sum the 85%. In the case of HEU-MET-INTER-001, we can observe that the most relevant nuclear data for Bretscher's method are the ^{235}U average number of delayed neutrons per fission ($\bar{\nu}_d$) and the elastic cross section of ^{56}Fe. For Chiba's method, we obtain a contribution for the $\bar{\nu}_d$ similar to Bretscher but, as we increase a, the contribution to the relative uncertainty of elastic reaction and its statistical error get lower and finally disappear of the main 85% contribution for $a = 20$. This type of phenomenon explains the smaller uncertainty to nuclear data in Chiba's method than the one in Bretscher's method. The contribution of $\bar{\nu}_d$ seems to be stable for all the cases, but we observe a smooth improvement of its statistical error with increasing a. For the reactors IEU-MET-FAST-007 and 010 we observe a very similar trend than in the previous reactor [6].

For MIX-COMP-FAST-005 reactor, the most relevant contributors to nuclear data uncertainty for Bretscher's method are the elastic cross section of ^{56}Fe, the $\bar{\nu}_d$ of ^{239}Pu and ^{238}U and the inelastic cross sections of ^{238}U, that remains even for high values of a, and hence seems to be a "real" effect, not due to poor statistics

---

[6]The $\bar{\nu}_d$ of ^{235}U and ^{238}U and the elastic cross section of ^{238}U are the most relevant contributors for Bretscher's method. In these cases, the influence of elastic cross sections in the 85% explanation of the uncertainty disappear beyond $a = 5$ and only the $\bar{\nu}_d$ influence remains. These results are available in [38].

(although we saw that, in general, elastic/inelastic cross sections are not a real influence in the β_{eff} uncertainty). Beyond $a = 5$, there is not a relevant contribution of elastic cross section of ^{56}Fe.

If we observe the sensitivity profiles of elastic cross section for ^{56}Fe for HEU-MET-INTER-001 in figure 5.2.3 (notice the different ranges in the vertical axis), we can see that the statistical uncertainty and the values of the sensitivity profiles decreases with the increasing value of a, which explain the loss of contribution in the total uncertainty due to nuclear data and the lower statistical errors.

To sum up, it has been observed that there is a clear problem of convergence (solved with Chiba's method for our benchmark reactors) with scattering (elastic and inelastic) with Bretscher's method, which causes that these reactions appear to have some influence when we try to weight the uncertainty to nuclear data in the delayed neutron fraction. This is an important effect to take into account when calculating β_{eff} by Bretscher's method.

Table 5.2.3: Evaluated reaction uncertainties due to nuclear data (and statistical error) of delayed neutron fraction of MIX-COMP-FAST-005 obtained for different cases. Uncertainty for the JENDL-4.0u library.

Case	MIX-COMP-FAST-005 uncertainties (%)			
	238U (n,n')	238U $\bar{\nu}_d$	56Fe (n,n)	239Pu $\bar{\nu}_d$
Bretscher	2 ± 3	1.895 ± 0.005	1.7 ± 2.4	1.5127 ± 0.0024
$a = 5$	1.32 ± 0.19	1.849 ± 0.003	-	1.5242 ± 0.0021
$a = 10$	1.14 ± 0.11	1.820 ± 0.003	-	1.5391 ± 0.0018
$a = 20$	1.16 ± 0.04	1.7689 ± 0.0022	-	1.5671 ± 0.0017

Table 5.2.4: Evaluated reaction uncertainties due to nuclear data (and statistical error) of delayed neutron fraction of HEU-MET-INTER-001 obtained for different cases. Uncertainty for the JENDL-4.0u library.

Case	HEU-MET-INTER-001 uncertainties (%)	
	235U $\bar{\nu}_d$	56Fe (n,n)
Bretscher	2.627 ± 0.004	2 ± 7
$a = 5$	2.621 ± 0.003	0.8 ± 1.0
$a = 10$	2.6240 ± 0.0022	0.3 ± 0.7
$a = 20$	2.6274 ± 0.0019	-

(a) SP for the β_{eff} due to ^{56}Fe cross section with Bretscher's method.

(b) SP for the β_{eff} due to ^{56}Fe cross section with $a = 5$.

(c) SP for the β_{eff} due to ^{56}Fe cross section with $a = 10$.

(d) SP for the β_{eff} due to ^{56}Fe cross section with $a = 20$.
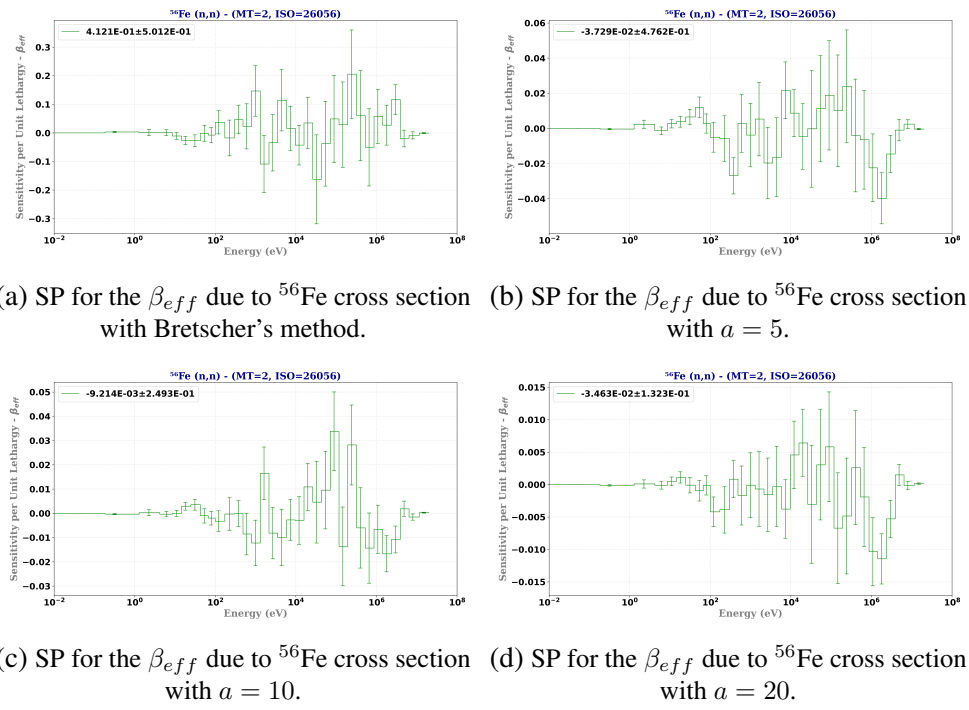
Figure 5.2.3: SP for the β_{eff} due to ^{56}Fe cross section for HEU-MET-INTER-001.

5.3 Statistical convergence of the results

In this subsection, we will check how is the accuracy of SUMMON for evaluating the statistical uncertainties of the uncertainties due to nuclear data. As stated above, sensitivity profiles calculated with Monte Carlo codes are affected by statistical errors, and these statistical errors affect the uncertainties due to nuclear data calculated by the sandwich rule. SUMMON propagates these errors using classical standard deviation propagation formulae. The actual formulae are however very complex due to the need of having to take into account all correlations between nuclear data [7].

To do this analysis, we have run ten simulations of HEU-MET-INTER-001 with different random seeds and ten times less statistics than in the simulations we performed in the rest of the section (to use a reasonable computational time in this part of the work). From these ten values, the (statistical) standard deviation of the uncertainty due to nuclear data can be calculated as:

$$std = \sqrt{\frac{\sum_i (u_i - \bar{u})^2}{N - 1}}, \tag{5.3.1}$$

where u denotes uncertainty due to nuclear data and $\bar{u}$ its mean value. In order to compare this statistical value with the evaluated by SUMMON for the original simulation, we have to divide it by additionally $\sqrt{10}$ (because there are ten simulations with ten times less statistic than the original simulation of HEU-MET-INTER-001).

---

[7]SUMMON version 2.2 has been used to explore/study this issue, since it has also been used for the S/U calculations.

Now, let us see the results in tables 5.3.1 and 5.3.2. In the total table we can observe the values for the statistical std of total uncertainties due to nuclear data for β_{eff}. In this case, there is a good agreement (up to a factor of two in the worst cases) between statistical uncertainties evaluated with SUMMON and the evaluated with the formulae (5.3.1), better for Chiba's method, for the better statistical convergence of this method 5.2.

In the contributions table, we can observe the values for the std of reaction contributions to the total uncertainty due to nuclear data. More discrepancies can be found here, for the three libraries and both methods, with differences that reach one order of magnitude. So, we can conclude that SUMMON has a high accuracy in the evaluation of statistical error of total uncertainty due to nuclear data, but it has some problems when obtaining statistical uncertainties in the reaction contributions, maybe due to internal programming of SUMMON or to the need of a larger sample to a better evaluation with equation (5.3.1).

Table 5.3.1: Statistical uncertainties of total uncertainties due to nuclear data for HEU-MET-INTER-001 evaluated with Eq. $(5.3.1)/\sqrt{10}$ and SUMMON v2.2

Case	Statistical unc. of total unc. due to nuclear data	
	Bretscher	Chiba
JEFF-3.3		
Eq. (5.3.1)	0.2194	0.01638
SUMMON	0.2128	0.01414
JENDL-4.0u		
Eq. (5.3.1)	0.1658	0.00453
SUMMON	0.1164	0.00510
ENDF/B-VIII.0		
Eq. (5.3.1)	0.0253	0.00170
SUMMON	0.0102	0.00212

Table 5.3.2: Statistical uncertainties of reaction contributions to total uncertainties due to nuclear data for HEU-MET-INTER-001 evaluated with Eq. $(5.3.1)/\sqrt{10}$ and SUMMON v2.2

Quantity	Statistical unc. of total unc. due to nuclear data			
	Bretscher		Chiba	
	Eq. (5.3.1)	SUMMON	Eq. (5.3.1)	SUMMON
JEFF-3.3				
235U (n,f)/235U (n,f)	0.0819	0.0889	0.00606	0.00532
235U χ/235U χ	0.3419	0.1385	0.02581	0.00286
JENDL-4.0u				
235U $\bar{\nu}_d$/235U $\bar{\nu}_d$	0.009665	0.002570	0.001067	0.001435
ENDF/B-VIII.0				
235U $\bar{\nu}_d$/235U $\bar{\nu}_d$	0.01594	0.00451	0.001486	0.002474

5.4 Reactions contribution and libraries comparison

In this subsection, we will show the most relevant reactions contributing to the uncertainty due to nuclear data in the multiplication factor and the delayed neutron fraction and how different libraries will lead us to different contributions from individual reactions. In the following tables for the reaction contributions, the pairs of nuclear data indicate the contribution due to the covariance between these nuclear data. The negative values indicate a negative contribution to the uncertainty due to nuclear data. Let us start with the multiplication factor.

5.4.1 Reactions contribution for k_{eff}

Even though we could see in subsection 5.1.1 that the convariance matrices of the JEFF library yield usually the largest nuclear data related uncertainties, the three libraries give us similar relevant reactions [8]. For the uranium systems, for which we have an example in table 5.4.1, we find fission cross section, spectrum (χ) and $\bar{\nu}_p$ and $\bar{\nu}$ of uranium isotopes. We can also find elastic and inelastic cross sections of ^{238}U and ^{235}U with low statistical error in the uncertainty due to nuclear data so, for the k_{eff}, their influence in this uncertainty must be taken into account. We can observe that the cross uncertainty $\bar{\nu}_p$ and $\bar{\nu}$ has a large statistical error. Another recurrent reaction that we can find is the radiative capture of ^{235}U and ^{238}U.

For the ^{239}Pu cores, for which we have an example in table 5.4.2, we can find very similar reactions than for the other cores, only that we change fission nuclear data of uranium for plutonium. We can find another relevant elastic scattering cross sections, as the one for ^{56}Fe and ^{52}Cr.

If we now observe the integrated sensitivity coefficients (ISCs) in energy for the multiplication factor in table 5.4.3 (SNEAK-7A), we can infer how the different nuclear data affect the k_{eff} in all the energy range. In general, we report positive ISCs for nuclear data related to fission, because this data is related with the generation of neutrons. The elastic and inelastic scattering cross sections have usually positive ISCs [9]. The only relevant reaction that is clearly negative is the radiative capture, a big rival of the fission reaction (remember that this reaction consist in the absorption of a neutron and the emission of a photon, so we lose a neutron without making new ones for the next generation). For the SNEAK-7A reactor case, we can compare our ISCs with the most relevant found in the paper [39] and we can observe a good agreement between them [10].

---

[8]The ^{235}U fission cross section appears less times in JENDL than in the others, maybe JENDL underestimates this reaction for reactor calculations (see reference [38]).

[9]Except in some fast reactors as MIX-COMP-FAST-005, IEU-MET-FAST-010, 020, 022 and SNEAK-7B, where there are some scattering reactions with negatives ISCs (see reference [38]).

[10]An interesting result can be found for the fission spectra nuclear data. In spite of having a negligible sensitivity profile, its uncertainty contribution is relevant in the three libraries.

Table 5.4.1: Reaction contribution to multiplication factor uncertainty due to nuclear data of IEU-MET-FAST-010. In brackets, % of the uncertainty explained by the showed reactions.

Quantity	$\Delta k_{eff}/k_{eff}$ (%)
JEFF-3.3 (83.9%)	
235U (n,f)/235U (n,f)	1.1542 ± 0.0011
235U χ/235U χ	0.8491 ± 0.0008
238U (n,n')/238U (n,n')	0.674 ± 0.008
JENDL-4.0u (90.7%)	
238U (n,n')/238U (n,n')	1.092 ± 0.004
235U χ/235U χ	0.54247 ± 0.00012
238U (n,γ)/238U (n,γ)	0.4715 ± 0.0003
ENDF/B-VIII.0 (73.0%)	
235U (n,f)/235U (n,f)	0.6174 ± 0.0005
238U (n,γ)/238U (n,γ)	0.44343 ± 0.00019
235U $\bar{\nu}$/235U $\bar{\nu}_p$	0.4 ± 0.6

Table 5.4.2: Reaction contribution to multiplication factor uncertainty due to nuclear data of PU-MET-INTER-002. In brackets, % of the uncertainty explained by the showed reactions.

Quantity	$\Delta k_{eff}/k_{eff}$ (%)
JEFF-3.3 (92.2%)	
239Pu (n,γ)/239Pu (n,γ)	0.8499 ± 0.0005
239Pu (n,f)/239Pu (n,f)	0.7168 ± 0.0008
239Pu $\bar{\nu}_p$/239Pu $\bar{\nu}_p$	0.46022 ± 0.00017
JENDL-4.0u (76.2%)	
56Fe (n,n)/56Fe (n,n)	0.392 ± 0.012
56Fe (n,γ)/56Fe (n,γ)	0.3447 ± 0.0003
239Pu (n,γ)/239Pu (n,γ)	0.32108 ± 0.00006
ENDF/B-VIII.0 (78.2%)	
239Pu $\bar{\nu}$/239Pu $\bar{\nu}$	0.26807 ± 0.00011
239Pu $\bar{\nu}_p$/239Pu $\bar{\nu}_p$	0.26745 ± 0.00011
52Cr(n,n)/52Cr(n,n)	0.211 ± 0.006

Table 5.4.3: ISCs for the multiplication factor of SNEAK-7A.

Quantity	Integrated Sensitivity Coefficients for k_{eff} (%/%)	
	MCNP	Kodeli, [39]
239Pu (n,f)	0.5485 ± 0.0003	0.54
239Pu $\bar{\nu}_p$	0.7955 ± 0.0003	0.779
238U $\bar{\nu}_p$	0.13257 ± 0.00009	0.137
239Pu $\bar{\nu}$	0.7971 ± 0.0003	-
239Pu χ	0.0000 ± 0.0003	-
238U (n,γ)	-0.16411 ± 0.00006	-
238U $\bar{\nu}$	0.13450 ± 0.00009	-

5.4.2 Reaction contribution for β_{eff}

Now, we are going to see and analyse the results for the delayed neutron fraction. In this case, major differences between libraries are found, as we can observe in some cases in tables from 5.4.4 to 5.4.6. For the delayed neutron fraction, the most relevant data, as expected, is $\bar{\nu}_d$. Having this in mind, we can classify the benchmark experiments in three groups: ^{233}U cores, for which there are covariance matrices for $\bar{\nu}_d$ in all three libraries; ^{235}U cores, for which there are covariance matrices for $\bar{\nu}_d$ in JENDL-4.0u and ENDF/B-VIII.0 but not in JEFF-3.3, and ^{239}Pu cores, for which there are covariance matrices for $\bar{\nu}_d$ only in JENDL-4.0u.

The reactions that appear in uncertainty tables are those that contribute to at least the 85% of the delayed neutron fraction uncertainty due to nuclear data. As we discussed in the former subsection 5.2, for the study of the most relevant reactions we must use the results for the Chiba's method, because of the problems with statistical convergence of the elastic/inelastic scattering reaction in Bretscher's method, which cause the appearance of these reactions as relevant due to very inaccurate sensitivity profiles. So, for the following analysis we will focus on the best library for each of the three groups and we only take in consideration the reactions that mainly contribute for Chiba's method.

For the singular case of U233-MET-FAST-006 the results with the three libraries are in very clear agreement (see table 5.4.4), more than the 85% of the total uncertainty due to nuclear data is explained with the $\bar{\nu}_d$ of the ^{233}U. If we have to choose one library of reference, we may take the JEFF in order to be conservative, because it provides us with the largest nuclear-data related uncertainties.

For the reactors with ^{235}U cores, we observe in the example of table 5.4.5 (IEU-MET-FAST-007) two main nuclear data that explain in general the 85% of the uncertainties, the $\bar{\nu}_d$ of ^{235}U and ^{238}U.

For the third group, ^{239}Pu systems, we can find in the example of table 5.4.6 (PU-MET-FAST-006) the $\bar{\nu}_d$ of ^{238}U and ^{239}Pu ($\bar{\nu}_d$ of ^{235}U is also included in the tables in order to compare with [39]). We can find in addition the contribution of the ^{238}U inelastic scattering cross section which, as we see in the subsection 5.2, is an exception of good convergence in the elastic/inelastic reactions, so we can consider it a real contributor to the total uncertainty due to nuclear data [11].

We have just observed that the suitability of the use of a library strongly depends on the materials of the core reactor, but the only one that in general provides good results of the most relevant reactions is JENDL because it includes the covariances of $\bar{\nu}_d$ for all major fissioning isotopes. For these three examples, we can compare with the results of [39] based on the JENDL-4.0u library and see a good agreement with the results shown in this paper [12].

If we take a look on the ISCs in the example of table 5.4.7 (SNEAK-7A), we can infer how this nuclear data affect to β_{eff} globally. Obviously, the ISCs of $\bar{\nu}_d$ are large and positive because it has a direct relation with β_{eff} [13]. The ISCs sign for the ^{238}U inelastic scattering cross section depends on the reactor design,

---

[11]We can also observe this for MIX-COMP-FAST-005, FCA-XIX-2, SNEAK-7A, 7B and MA-SURCA_ZONA2 reactors (see reference [38]).

[12]For PU-MET-FAST-001, HEU-MET-FAST-028, U233-MET-FAST-006, SNEAK-7A and 7B we have also a comparison with [39] with good agreement (see reference [38]).

[13]We can observe for SNEAK-7A and for MASURCA_ZONA2 similar ISCs for the $\bar{\nu}_d$ of ^{238}U and ^{239}Pu for each reactor (see reference [38]).

being negative in our example. We can observe large ISCs with large statistical uncertainties for elastic/inelastic scattering with Bretscher's method, but, when we observe the same ISCs evaluated with Chiba's method we find small ISCs with small statistical uncertainties (as we observed for the sensitivity profiles in 5.2), so these reaction have a negligible real influence to the β_{eff} uncertainty due to nuclear data. A remarkable issue is that the ISCs of $\bar{\nu}_p$ and $\bar{\nu}$ also show large values, usually with opposite sign that those of $\bar{\nu}_d$. The same behaviour was presented without explanation in [39]. Finally, we can observe in general a good agreement with this paper [39].

Table 5.4.4: Reaction contribution to delayed neutron fraction uncertainty due to nuclear data of U233-MET-FAST-006. All the reactions showed explain an 85% of the total uncertainty at least. The library used in [39] is JENDL-4.0m.

Quantity	$\Delta\beta_{eff}/\beta_{eff}$ (%)		
	Bretscher	Chiba	Kodeli, [39]
JEFF-3.3			
233U $\bar{\nu}_d$/233U $\bar{\nu}_d$	6.597 ± 0.019	6.576 ± 0.004	-
JENDL-4.0u			
233U $\bar{\nu}_d$/233U $\bar{\nu}_d$	5.213 ± 0.015	5.201 ± 0.004	5.097
ENDF/B-VIII.0			
233U $\bar{\nu}_d$/233U $\bar{\nu}_d$	5.213 ± 0.015	5.201 ± 0.004	-

Table 5.4.5: Reaction contribution to delayed neutron fraction uncertainty due to nuclear data of IEU-MET-FAST-007. All the reactions showed explain an 85% of the total uncertainty at least. The library used in [39] is JENDL-4.0m.

Quantity	$\Delta\beta_{eff}/\beta_{eff}$ (%)		
	Bretscher	Chiba	Kodeli, [39]
JEFF-3.3			
238U (n,n')/238U (n,n')	0.5 ± 1.9	0.31 ± 0.06	-
238U $\bar{\nu}_p$/238U $\bar{\nu}_p$	0.447 ± 0.023	0.4051 ± 0.0013	-
235U (n,f)/235U (n,f)	0.39 ± 0.14	0.316 ± 0.007	-
235U $\bar{\nu}_p$/238U $\bar{\nu}_p$	0.27 ± 0.03	-	-
235U χ/235U χ	-	0.406 ± 0.008	-
JENDL-4.0u			
235U $\bar{\nu}_d$/235U $\bar{\nu}_d$	1.8640 ± 0.0018	1.9739 ± 0.0012	1.8570
238U $\bar{\nu}_d$/238U $\bar{\nu}_d$	1.4815 ± 0.0023	1.3102 ± 0.0012	-
238U (n,n)/238U (n,n)	1.3 ± 0.7	-	-
ENDF/B-VIII.0			
235U $\bar{\nu}_d$/235U $\bar{\nu}_d$	2.5508 ± 0.0025	2.6686 ± 0.0017	-

Table 5.4.6: Reaction contribution to delayed neutron fraction uncertainty due to nuclear data of PU-MET-FAST-006. All the reactions showed explain an 85% of the total uncertainty at least. The library used in [39] is JENDL-4.0m.

Quantity	$\Delta\beta_{eff}/\beta_{eff}$ (%)		
	Bretscher	Chiba	Kodeli, [39]
JENDL-4.0u			
235U $\bar{\nu}_d$/235U $\bar{\nu}_d$	0.0637 ± 0.0004	0.0684 ± 0.0003	0.066
238U $\bar{\nu}_d$/238U $\bar{\nu}_d$	1.241 ± 0.007	1.1760 ± 0.0019	1.191
238U (n,n')/238U (n,n')	2.3 ± 0.8	1.80 ± 0.03	1.712
239Pu $\bar{\nu}_d$/239Pu $\bar{\nu}_d$	1.340 ± 0.005	1.3439 ± 0.0010	1.347

Table 5.4.7: ISCs for the delayed neutron fraction of SNEAK-7A.

Quantity	Integrated Sensitivity Coefficients for β_{eff} (%/%)		
	Bretscher	Chiba	Kodeli, [39]
238U (n,n')	-0.06 ± 0.12	-0.1548 ± 0.0017	-0.151
238U (n,f)	0.27 ± 0.04	0.261 ± 0.004	0.276
239Pu (n,f)	-0.21 ± 0.11	-0.224 ± 0.014	-0.252
238U $\bar{\nu}_d$	0.4967 ± 0.0021	0.4683 ± 0.0012	0.488
239Pu $\bar{\nu}_d$	0.4023 ± 0.0008	0.4117 ± 0.0014	0.402
238U $\bar{\nu}_p$	-0.25 ± 0.03	$-0.236308500 \pm 0.000000020$	-0.233
239Pu $\bar{\nu}_p$	-0.66 ± 0.10	-0.66953 ± 0.00003	-0.7
238U $\bar{\nu}$	0.25 ± 0.03	0.232 ± 0.004	0.255
239Pu $\bar{\nu}$	-0.26 ± 0.10	-0.258 ± 0.016	-0.298
238U (n,n)	-0.5 ± 0.3	0.00 ± 0.03	-
57Fe (n,n)	0.06 ± 0.04	0.000 ± 0.004	-
56Fe (n,n)	0.12 ± 0.17	-0.017 ± 0.017	-
238U χ	0.00 ± 0.03	0.000 ± 0.003	-
239Pu (n,n)	-0.14 ± 0.13	-0.006 ± 0.011	-
240Pu (n,n)	0.07 ± 0.04	-0.0006 ± 0.0008	-
240Pu (n,n')	0.014 ± 0.013	-0.0020 ± 0.0005	-
235U $\bar{\nu}_d$	0.05651 ± 0.00019	0.0594 ± 0.0006	-
239Pu χ	0.0 ± 0.1	0.000 ± 0.008	-

6   Conclusions

The major conclusions of this work are the following:

1. The uncertainty of the k_{eff} due to nuclear data has been found to be between 500 and 2000 pcm (0.5-2%) for the reactor systems analysed. The statistical uncertainty was about 1-4 pcm. This shows a clear dominance of the uncertainty due to nuclear data over the statistical uncertainty. In general, we observed larger relative uncertainties due to nuclear data for uranium systems than for plutonium systems (with the three libraries).

2. The delayed neutron fraction has been calculated with both Bretscher's and Chiba's methodologies. The first is expected to produce more accurate results while the second produces more precise results, since the second introduces a larger perturbation in the system. For this reason, an analysis of the biases introduced by Chiba's methodology has been performed and a good agreement between experimental and calculated values has been found for both Bretscher's and Chiba's methods, for the value of the perturbations used in this work.

3. Concerning the calculation of the uncertainty due to nuclear data, it has been found that Bretscher's method is affected by too large statistical errors to be practical, and hence Chiba's method is the preferred option. With Chiba's method, the uncertainty of β_{eff} due to nuclear data range between are between 1.15 and 32.8 pcm while statistical errors in our case are about 0.1 and 0.3 pcm, showing again a clear dominance of the uncertainty due to nuclear data. Statistical errors of the uncertainty due to nuclear data are between 0.004 and 0.7 pcm. Observing the data with JENDL library, there is not a clear separation between the relative uncertainties due to nuclear data of ^{235}U and plutonium systems, with the largest one for the ^{233}U system (a clear separation can be found in pcm, but this is due to the great difference between β_{eff} values for the different systems).

4. About the reactions with the largest contributions to the uncertainty, a wide range of reactions has been observed in the case k_{eff}, being fission, radiative capture and elastic/inelastic scattering of different nuclei the most relevant ones. The study of the ISCs has shown a positive influence of fission cross section and a negative influence of radiative capture on the k_{eff} value, while the sign of the influence of elastic and inelastic scattering depends on the reactor.

5. For β_{eff}, the largest contributor to the uncertainty due to nuclear data is the $\bar{\nu}_d$ of the major fissioning isotopes (^{233}U, ^{235}U, ^{238}U, ^{239}Pu), while inelastic scattering of ^{238}U also appears to be relevant in some reactors. The study of ISCs has shown a positive influence of $\bar{\nu}_d$ in the β_{eff} value, with negative or positive influence of inelastic scattering of ^{238}U depending on the the reactor. Furthermore, a negative and large influence of $\bar{\nu}_p$ from different fissionable nuclei has been observed, a fact that it is not explained at the moment.

6. Concerning the difference between libraries for S/U analyses, for the case of k_{eff} there is no obvious difference between the JEFF-3.3, ENDF-VIII.0 and JENDL-4.0u libraries, although JEFF-3.3 is the library that produces the largest uncertainties due to nuclear data in most reactors analysed. On the contrary, major differences between libraries have been observed in the case of S/U analyses of β_{eff}. The reason is the number of isotopes for which covariance matrices for $\bar{\nu}_d$ are included. The three libraries contain covariance matrices for $\bar{\nu}_d$ of ^{233}U, so all three can be used in the case of ^{233}U systems, with the JEFF-3.3 library providing the largest uncertainty due to nuclear data. ENDF/B-VIII.0 contains only covariance matrix of $\bar{\nu}_d$ of ^{235}U but only JENDL-4.0u contains the covariance matrices of $\bar{\nu}_d$ of ^{233}U, ^{235}U and ^{239}Pu. Hence, JENDL-4.0u is the most suitable library for S/U analyses in β_{eff}.

7. Finally, the quality of SUMMON (v2.2) procedures for propagating the statistical errors in the sensitivity profiles to the uncertainty in the nuclear data has been investigated. This has been achieved by performing Monte Carlo simulations with different random seeds. It has been found a good accuracy for the statistical error of the total uncertainty due to nuclear data for β_{eff}. On the other hand, we have observed large discrepancies, even of an order of magnitude, for the statistical errors of the contributions of individual reactions to the total uncertainty due to nuclear data.

Once we have shown and analysed our results, we can suggest different paths to continue this research:

1. With respect to SUMMON, it is necessary to check and improve the implementation of the Sandwich Rule for the evaluation of reaction contributions to the total uncertainty due to nuclear data; and maybe a revision of the different approximations carried out by the code in the statistical uncertainties calculations of the sensitivity profiles.

2. With respect to system and parameters, it would be interesting to perform the S/U analysis we have done for k_{eff} and β_{eff} with other reactor parameters, such as the mean generation time Λ. Furthermore, the analysis performed in this work can be extended to other types of reactors, as new designs of small modular reactors or accelerator driven systems as MYRRHA [40].

3. With respect to nuclear data, at least two major questions have arisen during this work that remain to be answered: the large negative influence of $\bar{\nu}_p$ (negative ISCs) in the sensitivity analysis of β_{eff} and the non-negligible influence of the fission spectra nuclear data in uncertainties due to nuclear data for the k_{eff}, despite the very small ISCs for both reactor parameters, that can be considered to be zero.

References

[1]   IAEA. *Country Nuclear Power Profiles: SPAIN*. IAEA, 2018.

[2]   United Nations Economic Commission for Europe. *Life Cycle Assessment of Electricity Generation Options*. United Nations, 2021.

[3]   H. Ritchie. *What are the safest and cleanest sources of energy?* `https://ourworldindata.org/safest-sources-of-energy`. 2020.

[4]   I. Kodeli P. Romojaro F. Alvarez-Velarde. "Nuclear data sensitivity and uncertainty analysis of effective neutron multiplication factor in various MYRRHA core configurations". In: *Annals of Nuclear Energy* (2016).

[5]   EC Community Research and Development Information Service. *CHANDA project*. `https://cordis.europa.eu/project/id/605203`. 2018.

[6]   V. Becares. *SANDA Project D5.1: Report on sensitivity analysis methods*. HORIZON 2020 RESEARCH and INNOVATION FRAMEWORK PROGRAMME OF THE EUROPEAN ATOMIC ENERGY COMMUNITY, 2018.

[7]   V. Bécares and F. Álvarez-Velarde et al. *SANDA T4.4 - Nuclear data evaluation and uncertainties. Applications*. `https://indico.cern.ch/event/999813/contributions/4205951/attachments/2187349/3696096/T4.4_SANDA_T4.4_GM2021_v3.1.pdf`. 2021.

[8]   NuPECC. *NuPECC Long Range Plan 2017 Perspectives in Nuclear Physics*. European Science Foundation, 2017.

[9]   P. Romojaro Otero. "Nuclear data analyses for improving the safety of advanced lead-cooled reactors". PhD thesis. Escuela Técnica Superior de Ingenieros Industriales, Universidad Politécnica de Madrid, 2019.

[10] N. Soppera, M. Bossant, and E. Dupont. "JANIS 4: An Improved Version of the NEA Java-based Nuclear Data Information System". In: *Nuclear Data Sheets* 120 (2014), pp. 294–296.

[11] R.E. MacFarlane. *An Introduction to the ENDF Formats*. Lectures given at the Workshop on Nuclear Data, Nuclear Reactors: Physics, Design, and Safety, 2000.

[12] M. Salvatores et al. "Nuclear waste transmutation". In: *Applied Radiation and Isotopes* 46.6 (1995), pp. 681–687. URL: `https://www.sciencedirect.com/science/article/pii/0969804395001336`.

[13] "Water cooled breeder program summary report (LWBR (Light Water Breeder Reactor) development program)". In: (Oct. 1987). URL: `https://www.osti.gov/biblio/6957197`.

[14] D. L. Hetrick. *Dynamics of Nuclear Reactors*. The University of Chicago Press, 1971.

[15] G. I. Bell and S. Glasstone. "Nuclear Reactor Theory". In: (Oct. 1970).

[16] D. G. Cacuci. *Volume I: SENSITIVITY and UNCERTAINTY ANALYSIS.* CHAPMAN HALL/CRC, 2003.

[17] A. Nouri, P. Nagel, J. Blair Briggs, and T. Ivanova. "DICE: Database for the International Criticality Safety Benchmark Evaluation Program Handbook". In: *Nuclear Science and Engineering* 145.1 (2003), pp. 11–19. DOI: 10.13182/NSE03-15. URL: https://doi.org/10.13182/NSE03-15.

[18] B. T. Rearden and M. A. Jessee (Eds.) *SCALE Code System. ORNL/TM-2005/39 Version 6.2.3.* Oak Ridge National Laboratory, 2018.

[19] R. Macfarlane et al. "The NJOY Nuclear Data Processing System, Version 2016". In: (Jan. 2017). URL: https://www.osti.gov/biblio/1338791.

[20] C.J. Werner. *MCNP6 User's Manual, Code version 6.2.* Los Alamos National Laboratory, 2017.

[21] G. Palmiotti et al. "Nuclear Data Target Accuracies for Generation-IV Systems Based on the Use of New Covariance Data". In: *Journal of The Korean Physical Society - J KOREAN PHYS SOC* 59 (Aug. 2011).

[22] M.M. Bretscher. "Perturbation-Independent Methods for Calculating Research Reactor Kinetic Parameters". In: *Argonne National Laboratory* (1997).

[23] G. Chiba. "Calculation of Effective Delayed Neutron Fraction Using a Modified k-Ratio Method". In: *J. Nucl. Sci. Technol.* 46 (2009), 399–402.

[24] H. Iwamoto et al. "Monte Carlo uncertainty quantification of the effective delayed neutron fraction". In: *Journal of Nuclear Science and Technology* 55.5 (2018), pp. 539–547.

[25] H. C. Paxton. *A History of Critical Experiments at Pajarito Site.* Los Alamos National Laboratory, 1983.

[26] Nuclear Energy Agency. "ICSBEP Handbook 2020". In: (2020). URL: https://www.oecd-ilibrary.org/content/data/7e0ebc50-en.

[27] Nuclear Energy Agency. "IRPhe Handbook 2020". In: (2020). URL: https://www.oecd-ilibrary.org/content/data/d863e360-en.

[28] I. Hill, N. Soppera, and M. Bossant. "IDAT: The International Handbook of Evaluated Reactor Physics Benchmark Experiments Database and Analysis Tool". In: *Nuclear Science and Engineering* 178.3 (2014), pp. 280–294.

[29] S. Okajima et al. "Summary on international benchmark experiments for effective delayed neutron fraction (β_{eff})". In: *Progress in Nuclear Energy* 41.1-4 (2002), pp. 285–301.

[30] J. Leppanen et al. "Calculation of effective point kinetics parameters in the Serpent 2 Monte Carlo code". In: *Annals of Nuclear Energy* 65 (2014), pp. 272–279.

[31] R. K. Meulekamp and S. C. van der Marck. "Calculating the Effective Delayed Neutron Fraction with Monte Carlo". In: *Nuclear Science and Engineering* 152.2 (2006), pp. 142–148.

[32] E. F. Bennett. *An experimental method for reactor-noise measurements of effective beta*. Argonne National Laboratory, 1981.

[33] K. Nakajima. "Re-evaluation of the Effective Delayed Neutron Fraction Measured by the Substitution Technique for a Light Water Moderated Low-enriched Uranium Core". In: *Journal of Nuclear Science and Technology* 38.12 (2001), pp. 1120–1125.

[34] G. S. Brunson et al. *A survey of prompt-neutron lifetimes in fast critical systems*. Argonne National Laboratory, 1963.

[35] T. Sakurai et al. "Measurement of effective delayed neutron fraction eff by covariance-to-mean method for benchmark experiments of eff at FCA". In: *Progress in Nuclear Energy* 35.2 (1999), pp. 203–208.

[36] J. L. de Francisco. *Determinación de la fracción efectiva de neutrones retardados en el Reactor Coral-1*. Junta de Energía Nuclear, 1973.

[37] S. G. Carpenter, J. M. Gasidlo, and J. M. Stevenson. "Measurements of the Effective Delayed-Neutron Fraction in Two Fast Critical Experiments". In: *Nuclear Science and Engineering* 49.2 (1972), pp. 236–239.

[38] `https://github.com/VicenteBecares/Propagation-of-errors-in-nuclear-data-to-reactor-parameters`.

[39] I. Kodeli. "Sensitivity and uncertainty in the effective delayed neutron fraction (β_{eff})". In: *Nuclear Instruments and Methods in Physics Research A* 715 (2013), pp. 70–78.

[40] International team of experts. *Independent evaluation of the MYRRHA project*. OECD Nuclear Energy Agency, 2009.

A Values of k_{eff}, β_{eff} and their uncertainties

Table A.1: Multiplication factor k_{eff} and total uncertainties for each reactor.

Benchmark	k_{eff}^{exp}	$k_{eff}^{MCNP}\pm$ Stat. Unc.	Unc. to Data$\pm$ Stat. Unc.		
			JEFF-3.3	JENDL-4.0u	ENDF/B-VIII.0
HEU-MET -INTER- 001	0.997 $\pm$ 0.003	1.01018 $\pm$ 0.00002	0.018268 $\pm$ 0.000019	0.00935 $\pm$ 0.00005	0.013770 $\pm$ 0.000011
MIX-COMP -FAST- 005	0.9913 $\pm$ 0.0023	0.99255 $\pm$ 0.00001	0.009689 $\pm$ 0.000011	0.008910 $\pm$ 0.000015	0.006152 $\pm$ 0.000006
PU-MET -INTER- 002	0.9878 $\pm$ 0.0023	1.00259 $\pm$ 0.00002	0.01309 $\pm$ 0.00011	0.00806 $\pm$ 0.00004	0.005552 $\pm$ 0.000022
PU-MET -INTER- 004	0.9723 $\pm$ 0.0025	0.97378 $\pm$ 0.00002	0.009692 $\pm$ 0.000011	0.006823 $\pm$ 0.000015	0.006380 $\pm$ 0.000020
IEU-MET -FAST- 010	0.9954 $\pm$ 0.0024	0.99735 $\pm$ 0.00002	0.018810 $\pm$ 0.000021	0.01437 $\pm$ 0.00003	0.006380 $\pm$ 0.000020
IEU-MET -FAST- 020	1.002 $\pm$ 0.0013	1.00562 $\pm$ 0.00001	0.015714 $\pm$ 0.000008	0.008200 $\pm$ 0.000012	0.010980 $\pm$ 0.000004
IEU-MET -FAST- 021	1.0084 $\pm$ 0.0015	1.01149 $\pm$ 0.00001	0.016834 $\pm$ 0.000009	0.010713 $\pm$ 0.000019	0.012207 $\pm$ 0.000011
IEU-MET -FAST- 022	1.0008 $\pm$ 0.0013	1.00233 $\pm$ 0.00001	0.016435 $\pm$ 0.000007	0.007472 $\pm$ 0.000010	0.011107 $\pm$ 0.000003
LEU-COMP -THERM- 006	1.0000 $\pm$ 0.0025	1.00072 $\pm$ 0.00001	0.008652 $\pm$ 0.000004	0.007082 $\pm$ 0.000003	0.0091990 $\pm$ 0.0000011
LEU-COMP -THERM- 067	1.0005 $\pm$ 0.0005	1.00163 $\pm$ 0.00004	0.00907 $\pm$ 0.00008	0.00771 $\pm$ 0.00009	0.01007 $\pm$ 0.00006
PU-MET -FAST- 001	1.000 $\pm$ 0.004	0.99929 $\pm$ 0.00001	0.006881 $\pm$ 0.000004	0.0073271 $\pm$ 0.0000019	0.013770 $\pm$ 0.000011
IEU-MET -FAST- 007	1.0045 $\pm$ 0.0007	1.00493 $\pm$ 0.00001	0.018049 $\pm$ 0.000010	0.013764 $\pm$ 0.000017	0.011716 $\pm$ 0.000006
PU-MET -FAST- 006	1.000 $\pm$ 0.003	1.00335 $\pm$ 0.00002	0.009819 $\pm$ 0.000011	0.008137 $\pm$ 0.000009	0.007409 $\pm$ 0.000009

Table A.2: Multiplication factor k_{eff} and total uncertainties for each reactor.

Benchmark	k_{eff}^{exp}	$k_{eff}^{MCNP}\pm$ Stat. Unc.	Unc. to Data$\pm$ Stat. Unc.		
			JEFF-3.3	JENDL-4.0u	ENDF/B-VIII.0
U233-MET -FAST- 006	1.0000 ± 0.0014	1.00337 ± 0.00002	0.010679 ± 0.000008	0.011407 ± 0.000007	0.011621 ± 0.000006
HEU-MET -FAST- 001	1.0000 ± 0.0010	1.00013 ± 0.00001	0.013189 ± 0.000010	0.010413 ± 0.000012	0.012084 ± 0.000003
HEU-MET -FAST- 028	1.000 ± 0.003	1.00412 ± 0.00001	0.014152 ± 0.000009	0.008806 ± 0.000011	0.012332 ± 0.000006
FCA -XIX- 1	-	1.00761 ± 0.00002	0.014593 ± 0.000007	0.008627 ± 0.000009	0.013061 ± 0.000004
FCA -XIX- 2	-	1.21884 ± 0.00002	0.008631 ± 0.000009	0.007346 ± 0.000013	0.005784 ± 0.000008
FCA -XIX- 3	-	0.99441 ± 0.00002	0.007109 ± 0.000013	0.00669 ± 0.00003	0.005306 ± 0.000022
SNEAK-7A	-	1.0095 ± 0.00002	0.008618 ± 0.000010	0.007185 ± 0.000015	0.005619 ± 0.000008
SNEAK-7B	-	1.00488 ± 0.00001	0.010033 ± 0.000011	0.009633 ± 0.000019	0.006579 ± 0.000007
MASUR- CA_ R2	-	0.99246 ± 0.00002	0.01658 ± 0.00011	0.00703 ± 0.00008	0.01207 ± 0.00008
MASUR- CA_ ZONA2	-	1.00309 ± 0.00002	0.00813 ± 0.00009	0.00689 ± 0.00007	0.00522 ± 0.00005
HEU-MET -FAST- 062	0.9987 ± 0.0010	1.00338 ± 0.00002	0.013792 ± 0.000012	0.008211 ± 0.000013	0.011923 ± 0.000008
HEU-MET -FAST- 100	1.0026 ± 0.0007	1.00412 ± 0.00001	0.013210 ± 0.000010	0.010373 ± 0.000012	0.012097 ± 0.000004

Table A.3: Delayed neutron fraction β_{eff} and total uncertainties for each reactor. In the top of each row, the β_{eff} and uncertainty calculated by Bretscher's method are found, and in the bottom, by Chiba's method.

Benchmark	β_{eff}^{exp} (pcm)	$\beta_{eff}^{eval} \pm$ Stat. Unc. (pcm)	Unc. to Data $\pm$ Stat. Unc. (pcm)		
			JEFF-3.3	JENDL-4.0u	ENDF/B-VIII.0
HEU-MET -INTER- 001	659 ± 13	682 ± 3	32 ± 6	27 ± 5	34.7 ± 1.9
		684.20 ± 0.10	4.47 ± 0.12	18.22 ± 0.04	31.208 ± 0.021
MIX-COMP -FAST- 005	381 ± 8	387.9 ± 1.4	9.3 ± 1.9	15.9 ± 2.2	8 ± 3
		375.60 ± 0.10	$5.1 \ pm \ 0.1$	10.86 ± 0.07	4.34 ± 0.05
PU-MET -INTER- 002	222 ± 4	234 ± 3	22 ± 4	29 ± 8	18 ± 4
		233.10 ± 0.10	1.79 ± 0.15	11.32 ± 0.07	1.35 ± 0.22
PU-MET -INTER- 004	223 ± 10	250 ± 3	10.7 ± 1.8	14.2 ± 1.7	15 ± 4
		248.60 ± 0.10	1.88 ± 0.10	10.386 ± 0.017	1.35 ± 0.09
IEU-MET -FAST- 010	725 ± 15	738 ± 3	11 ± 3	21 ± 3	22.1 ± 2.4
		713.60 ± 0.20	6.06 ± 0.21	18.21 ± 0.07	19.95 ± 0.03

Table A.4: Delayed neutron fraction β_{eff} and total uncertainties for each reactor. In the top of each row, the β_{eff} and uncertainty calculated by Bretscher's method are found, and in the bottom, by Chiba's method.

Benchmark	β_{eff}^{exp} (pcm)	$\beta_{eff}^{eval}\pm$ Stat. Unc. (pcm)	Unc. to Data± Stat. Unc. (pcm)		
			JEFF-3.3	JENDL-4.0u	ENDF/B-VIII.0
IEU-MET -FAST- 020	$(7.7 \pm 0.5) \cdot 10^1$	746.8±1.4	7.8 ± 1.5	22.4 ± 1.9	23.4 ± 1.0
		728.20±0.10	5.02 ± 0.07	18.04 ± 0.03	22.954 ± 0.012
IEU-MET -FAST- 021	$(7.7 \pm 0.5) \cdot 10^1$	750.3±1.4	6.7 ± 1.4	21.0 ± 2.0	22.6 ± 0.4
		732.20±0.10	5.54 ± 0.08	18.53 ± 0.05	21.977 ± 0.011
IEU-MET -FAST- 022	$(7.7 \pm 0.5) \cdot 10^1$	750.3±1.4	9.0 ± 2.0	19.7 ± 1.2	23.8 ± 0.3
		728.40±0.10	5.15 ± 0.07	17.66 ± 0.03	23.768 ± 0.012
LEU-COMP -THERM- 006	771±19	795.4±1.4	5.3 ± 0.7	22.24 ± 0.16	30.15 ± 0.06
		787.60±0.10	4.96 ± 0.04	21.928 ± 0.009	30.021 ± 0.009
LEU-COMP -THERM- 067	750±19	774.7±4.4	6 ± 6	23 ± 5	31 ± 11
		767.3±0.3	4.6 ± 0.3	22.13 ± 0.19	30.47 ± 0.19

Table A.5: Delayed neutron fraction β_{eff} and total uncertainties for each reactor. In the top of each row, the β_{eff} and uncertainty calculated by Bretscher's method are found, and in the bottom, by Chiba's method.

Benchmark	β_{eff}^{exp} (pcm)	$\beta_{eff}^{eval} \pm$ Stat. Unc. (pcm)	Unc. to Data$\pm$ Stat. Unc. (pcm)		
			JEFF-3.3	JENDL-4.0u	ENDF/B-VIII.0
PU-MET -FAST- 001	194±10	188.1±1.4	1.8 ± 0.4	4.58 ± 0.07	1.14 ± 0.12
		188.50±0.10	1.53 ± 0.04	4.529 ± 0.004	1.150 ± 0.007
IEU-MET -FAST- 007	720±7	739.4±1.4	6.9 ± 2.0	21 ± 3	20.5 ± 0.5
		714.90±0.10	5.69 ± 0.10	18.21 ± 0.04	20.058 ± 0.011
PU-MET- -FAST- 006	276±7	287±3	4.0 ± 1.6	9.2 ± 1.5	4.1 ± 0.7
		284.10±0.10	3.15 ± 0.07	7.74 ± 0.06	2.02 ± 0.04
U233-MET -FAST- 006	360±14	376±3	25.6 ± 0.6	21.6 ± 0.6	20.5 ± 0.3
		374.30±0.10	24.853 ± 0.018	20.94 ± 0.03	19.965 ± 0.016
HEU-MET -FAST- 001	659±10	650.9±1.4	8.9 ± 1.4	19.2 ± 0.8	29.46 ± 0.07
		648.00±0.10	9.14 ± 0.09	19.02 ± 0.03	29.748 ± 0.014

Table A.6: Delayed neutron fraction β_{eff} and total uncertainties for each reactor. In the top of each row, the β_{eff} and uncertainty calculated by Bretscher's method are found, and in the bottom, by Chiba's method.

Benchmark	β_{eff}^{exp} (pcm)	$\beta_{eff}^{eval}\pm$ Stat. Unc. (pcm)	Unc. to Data$\pm$ Stat. Unc. (pcm)		
			JEFF-3.3	JENDL-4.0u	ENDF/B-VIII.0
HEU-MET -FAST- 028	675 ± 13	692.1 ± 1.4	9.4 $\pm$ 1.8	22.2 $\pm$ 1.7	27.1 $\pm$ 0.3
		687.20 ± 0.10	6.99 $\pm$ 0.07	18.41 $\pm$ 0.03	27.353 $\pm$ 0.013
FCA -XIX- 1	742 ± 24	764.2 ± 2.8	14.4 $\pm$ 2.3	22.3 $\pm$ 1.7	34.1 $\pm$ 0.5
		760.10 ± 0.20	4.45 $\pm$ 0.05	18.591 $\pm$ 0.021	32.760 $\pm$ 0.022
FCA -XIX- 2	364 ± 9	362.6 ± 2.3	13 $\pm$ 3	16 $\pm$ 4	11 $\pm$ 3
		357.10 ± 0.10	3.83 $\pm$ 0.13	8.72 $\pm$ 0.06	3.79 $\pm$ 0.04
FCA -XIX- 3	251 ± 4	256 ± 3	17 $\pm$ 4	16 $\pm$ 4	9 $\pm$ 3
		257.80 ± 0.10	1.69 $\pm$ 0.12	7.05 $\pm$ 0.06	1.67 $\pm$ 0.08
SNEAK-7A	$(40\pm3)\cdot10$	387 ± 3	7 $\pm$ 3	16 $\pm$ 4	8.3 $\pm$ 1.9
		372.40 ± 0.10	5.46 $\pm$ 0.14	10.84 $\pm$ 0.08	3.80 $\pm$ 0.05

Table A.7: Delayed neutron fraction β_{eff} and total uncertainties for each reactor. In the top of each row, the β_{eff} and uncertainty calculated by Bretscher's method are found, and in the bottom, by Chiba's method.

Benchmark	β_{eff}^{exp} (pcm)	$\beta_{eff}^{eval}\pm$ Stat. Unc. (pcm)	Unc. to Data± Stat. Unc. (pcm)		
			JEFF-3.3	JENDL-4.0u	ENDF/B-VIII.0
SNEAK-7B	$(44.0 \pm 3.4) \cdot 10$	437.9±1.4	10.0 ± 2.1	19 ± 4	8.6 ± 2.3
		417.60±0.10	5.53 ± 0.15	11.95 ± 0.10	5.14 ± 0.05
MASURCA _R2	721±11	740±3	14 ± 11	25 ± 10	28 ± 8
		727.20±0.20	4.5 ± 0.7	17.7 ± 0.4	26.4 ± 0.7
MASURCA _ZONA2	349±6	352.9±2.8	9 ± 12	15 ± 10	9 ± 8
		345.40±0.10	4.1 ± 0.6	9.13 ± 0.18	3.2 ± 0.7
HEU-MET -FAST- 062	663±17	7'00±3	12.7 ± 2.5	19.5 ± 1.1	27.31 ± 0.13
		687.50±0.20	6.71 ± 0.09	18.36 ± 0.04	27.295 ± 0.018
HEU-MET -FAST- 100	657±9	646.3±1.4	11.0 ± 2.0	18.9 ± 0.6	29.41 ± 0.07
		648.60±0.10	9.00 ± 0.09	18.98 ± 0.03	29.710 ± 0.013